Science of the Total Environment 878 (2023) 163163

Contents lists available at ScienceDirect

Science of the Total Environment

journal homepage: www.elsevier.com/locate/scitotenv

Comparative 6 + studies of environmentally persistent free radicals on nano-sized coal dusts

Sikandar Azam [a], Vasily Kurashov [b], John H. Golbeck [b], Sekhar Bhattacharyya [a], Siyang Zheng [c], Shimin Liu [a,*]

[a] Department of Energy and Mineral Engineering, G³ Center and Energy Institute, The Pennsylvania State University, University Park, PA 16802, USA
[b] Department of Chemistry, Pennsylvania State University, University Park, PA 16802, USA
[c] Department of Biomedical Engineering, College of Engineering, Carnegie Mellon University, 15213, USA

HIGHLIGHTS

- Coal dust contains free radicals in extremely large quantities.
- They can remain stable for several months to years and hence should be called as EPFRs.
- EPFRs in coal dust are mainly oxygenated and carbon-centered.
- EPFRs quantity (spin counts) increases with the carbon content and reflectance.
- EPFRs in the coal dust might be playing a major role in modulating the coal dust toxicity.

GRAPHICAL ABSTRACT

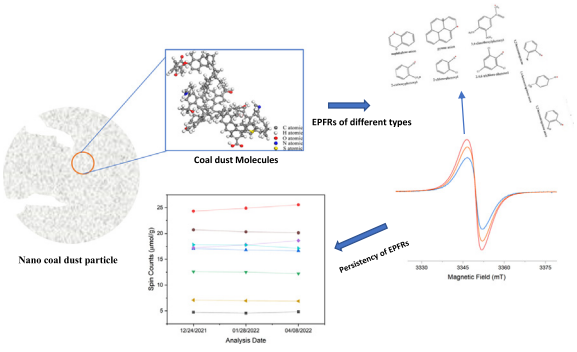

ARTICLE INFO

Editor: Pavlos Kassomenos

Keywords:
Environmentally persistent free radicals (EPFRs)
Coal dust
EPR
Toxicity
Black lung
Pneumoconiosis

ABSTRACT

Coal dust is the major hazardous pollutant in the coal mining environment. Recently environmentally persistent free radicals (EPFRs) were identified as one of the key characteristics which could impart toxicity to the particulates released into the environment. The present study used Electron Paramagnetic Resonance (EPR) spectroscopy to analyze the characteristics of EPFRs present in different types of nano-size coal dust. Further, it analyzed the stability of the free radicals in the respirable nano-size coal dust and compared their characteristics in terms of EPR parameters (spin counts and g-values). It was found that free radicals in coal are remarkably stable (can remain intact for several months). Also, Most of the EPFRs in the coal dust particles are either oxygenated carbon centered or a mixture of carbon and oxygen-centered free radicals. EPFRs concentration in the coal dust was found to be proportional to the carbon content of coal. The characteristic g-values were found to be inversely related to the carbon content of coal dust. The spin concentrations in the lignite coal dust were between 3.819 and 7.089 μmol/g, whereas the g-values ranged from 2.00352 to 2.00363. The spin concentrations in the bituminous coal dust were between 11.614 and 25.562 μmol/g, whereas the g-values ranged from 2.00295 to 2.00319. The characteristics of EPFRs present in coal dust identified by this study are similar to the EPFRs, which were found in other environmental pollutants such as combustion-generated particulates, $PM_{2.5}$, indoor dust, wildfires, biochar, haze etc., in some of the previous studies. Considering the toxicity analysis of environmental particulates containing EPFRs similar to those identified in the present study, it can be confidently hypothesized that the EPFRs in the coal dust might play a major role in modulating the coal dust toxicity. Hence, it is recommended that future studies should analyze the role of EPFR-loaded coal dust in mediating the inhalation toxicity of coal dust.

* Corresponding author at: Department of Energy and Mineral Engineering, Pennsylvania State University, 224 Hosler Building, University Park, PA 16802, USA.
E-mail address: szl3@psu.edu (S. Liu).

http://dx.doi.org/10.1016/j.scitotenv.2023.163163
Received 27 January 2023; Received in revised form 23 March 2023; Accepted 26 March 2023
Available online 31 March 2023

1. Background

One major health and its derivative issues of coal mining is workers' dust exposure, leading to respiratory diseases and health problems (Laney and Weissman, 2014). Any coal mining process, whether coal cutting, transportation or preparation processes, is associated with emitting and transporting dust particulates. In the past several years, it has been proven that coal dust is responsible for conditions such as chronic obstructive pulmonary disease (COPD), asthma, stunted lung development, cardiac arrhythmias, pneumoconiosis, acute myocardial infarction, and lung cancer (Petsonk et al., 2013). The coal mine workers prolonged interaction with the coal dust during the coal mining processes makes them highly susceptible to even serious forms of diseases such as coal workers' pneumoconiosis (CWP) and progressive massive fibrosis (PMF) (Laney and Weissman, 2014). Moreover, a spectrum of respiratory diseases collectively called "Coal Mine Dust Lung Disease (CMDLD)" is found to be associated with coal mine dust exposure (Laney and Weissman, 2014).

Coal dust exposure and its associated health impact are long associated with the coal mining industry. There is a long history of regulations and development to protect coal mine workers from coal dust-related health problems (Liu and Liu, 2020). Due to the progressive adaption of engineering dust control measures and the enforcement of dust regulation, there was good progress till 2000 in continuously decreasing dust-related occupational health issues. However, despite the laws and regulations limiting coal workers' exposure to coal dust, a resurgence of the disease was observed in 2003 in the U.S., one of the world's major coal-mining countries. A recent CDC/NIOSH report demonstrated that starting in 1995, the prevalence of CWP in U.S. underground coal miners had again begun to increase (Attfield et al., 2011). The most disturbing is the increase in severity, particularly among young miners in the Appalachian basin (of which the CWP prevalence is four times higher than the national average)—including Pennsylvania, West Virginia, Virginia, and Ohio (Doney et al., 2019; Hall et al., 2019). A dramatic increase in the prevalence of PMF among working underground coal miners has been observed in central Appalachia past decade (Fan and Liu, 2021). Not only in U.S. similar increase has been observed in other major coal-producing countries also, such as China and Australia (Liu and Liu, 2020).

These discussions and evidence suggest that the causes of coal dust toxicity remain unclear due to the complexity of the dust characteristics and its interactions with the human lung. Given workers' importance and level of involvement in the coal mining industry, there is a dire need to understand the characteristics and mediators of coal dust toxicity. Several reasons and characteristics of coal and other dust have been discussed in the literature to impact the toxic potential of coal dust. Some of these characteristics are silica content (Pavan et al., 2020), metal or metallic ions (Li and Liao, 2018; Li et al., 2018), particle size (Liu and Liu, 2020; R. Zhang et al., 2021), surface area (R. Zhang et al., 2021), wettability (Löndahl et al., 2010), pyrite content (Cohn et al., 2006), oxidative stress generating potential (Batool et al., 2020; Zazouli et al., 2021) and Free Radicals (FRs) (Dalal et al., 1995) etc. Recently, free radicals, which could persist in the environment for days to years, termed environmentally persistent free radicals (EPFRs), have received considerable attention as biological and environmentally hazardous substances. EPFRs are the species with free electrons in their configuration and can remain stable for more than one day, which could be detected with the help of Electron Paramagnetic Resonance (EPR) spectroscopy (Arangio et al., 2016). Their longer lifetime allows them to remain intact in the atmosphere longer and get transported farther distances. These characteristics overall affect the higher risk of EPFR exposure. While remaining intact during their transportation, combined with their reactive nature, EPFRs represent reservoirs of reactivity in the environment that influence the nature and toxic potential of the particulates (Filippi et al., 2022). Although there has been an ongoing discussion on EPFRs for more than half a century, their health impacts are poorly understood. Recently, there has been a surge in the number of studies attempting to understand the hidden reactions in the environmental systems, such as aerosols, cloud-condensation nuclei (CCN), and nano-scale reactions in the atmosphere aerosol toxicity. There is a clear increasing trend in research on the characterization and health effects of EPFRs present on environmental matrices, aerosols, nanoparticles, etc.

A study published in *Particle and Fibre Toxicology* raised biological concerns about the EPFRs in MCP230 due to their ability to induce lipid peroxidation (Balakrishna et al., 2009). This means that EPFRs in the ultrafine particles could modulate their cellular oxidative stress and cytotoxicity potentials. Another study demonstrated that the upper respiratory tract has the highest EPFR exposure and that the particle size could influence their potential toxicity (Chen et al., 2020). Another prominent mediator of particle toxicity is the potential of EPFRs to generate an overwhelming amount of reactive oxygen species (ROS), which leads to oxidative stress (Gurgueira et al., 2002; Okayama et al., 2006). There are many kinds of ROS reported in the particle phase, such as •R, •RO, $•RO_2$, •OH, $HO_2•$ etc. (Pavlovic and Hopke, 2010). Among these, •OH is the most damaging, and a recent study shows that the EPFRs in the $PM_{2.5}$ could generate hydroxyl radicals (Gehling et al., 2014). Another similar experimental observation calculated that one EPFR could generate ~10 hydroxyl free radicals (Khachatryan et al., 2011). Filippi et al. found a significant level of EPFRs from the particulate matter, dust and surfaces collected from the indoor environment from several locations (Filippi et al., 2022). Evidence suggests that the environmentally persistent free radicals (EPFRs) associated with PM can generate ROS because their redox-cycling nature leads to adverse health effects (Dellinger et al., 2001; Squadrito et al., 2001). A significant amount of EPFRs was observed in the $PM_{2.5}$ particles collected from the highway, which was linked with the ROS generation and total DTT activities at the highway sites (Hwang et al., 2021). The toxic effects of EPFRs are also observed, leading to adverse infant respiratory health effects (Saravia et al., 2013). Overall, the collective evidence suggests the potential toxicity mediating effect of acute and chronic exposure to EPFRs on atmospheric particles (Balakrishna et al., 2009; Saravia et al., 2013; Wang et al., 2011).

Research on the free radicals in coal and coal dust has been reported in the literature. Previous studies have characterized the free radicals present in the coal and coal conversion processes (Zhou et al., 2019). As early as 1968, Retcofsky made an EPR study on a series of American coal samples of peat, lignite, sub-bituminous, bituminous, and anthracitic to understand the chemistry and structure of coal. Pilawa et al. used EPR spectroscopy to characterize paramagnetic centers of reductively methylated and butylated Polish flame coal (70.8 wt% C) in a potassium–liquid ammonia system (Pilawa et al., 1998). Several other studies have used EPR spectroscopy to characterize coal (Dalal et al., 1989; Green et al., 2012) or understand the role of free radicals in several processes associated with coal utilization (Y. Zhang et al., 2021; Zhao et al., 2020).

As discussed earlier, coal dust toxicity is a serious occupational hazard, especially to the miners who are chronically exposed to it. There is a lack of studies demonstrating the role of EPFRs present in the coal dust in mediating its toxicity. The situation becomes more warranting when there is a reported increase in the coal dust-related health issues showing the limited understanding of the coal dust characteristics mediating its toxicity. Based on the reported literature, it was recognized that the EPFRs present in coal is widely recognized, but their effect in mediating coal dust toxicity has not been fully investigated and understood. As an analog, it is evidenced that the toxicity of the atmospheric particles increases with known EPFRs. We identified the need for improved understanding the role of the EPFRS in coal dust-induced toxicity and its implication to the recent surge in CWP in central Appalachia. Strong evidence suggests that the EPFRs could strongly mediate coal dust-induced induced CWP. Remarkably, stable coal radicals were detected and measured in the lungs of 98 coal miners, and free radicals were found in the autopsied coal miner's lungs (Dalal et al., 1991). They measured the stable radical concentrations from the lung tissue of 98 coal workers with and without (a) CWP, (b) cancer, and (c) a history of cigarette smoking (Dalal et al., 1991). The stable radical concentration was found to be related to the longer mining tenure and CWP disease severity. An increase in the stable free radical concentration was associated with the CWP severity (Dalal et al., 1991). Higher

concentrations of EPFRs were associated with workers working longer in central Pennsylvania's anthracite region. Moreover, the severity of CWP was well correlated with the progressive increase in free radical concentration. Something very important to note here is that the free radicals in coal dust are so stable that they were detected in the autopsied coal mine workers (dead man's lungs) that too in concentration slightly less than what was found for the nano-sized lignite coal dust in the present study (0.9 to 1.66 μmol/g). This study is strong evidence that EPFRs in coal have strong implications for their toxic potential.

Previous studies demonstrate that the coal dust-induced toxicity attributed to EPFRs is well correlated among long-term coal miners. This study provides direct measurements of EPFRs in different types of coal dust. The outcomes of this study offer a data set of the EPFRs in different ranks of coal and serve as the baseline for future toxicity studies. Several coal dust samples prepared from a range of lignite to bituminous coal were used for EPR spectroscopy. The data collected from EPR spectroscopy were processed to get the important EPR parameters further correlated with the several coal dust characterizations. The nature and quantity of the EPFRs obtained in this study strong findings beneficial for future biological tests for ultimate toxicity analysis. This research presents a unique way to understand coal dust toxicity issues and develop preventive measures.

2. Methods

2.1. Coal samples and their characteristics

Eight different types of coals were obtained from the Penn State Coal sample bank. The description of coal samples is provided in the supplementary sheet Table S1. This work aims to comprehensively investigate the EPFRs on coal with an expected implication on the mine workers' long-term health effects. In the United States, the most produced coal in tonnage is lignite and bituminous. Therefore, we choose two ranks, lignite and bituminous coals. We chose more bituminous coal samples (6 samples) because of the recent increasing trend of lung disease in the bituminous coal region, especially in the central Appalachian basin (Fan and Liu, 2021). As can be observed that the coal samples consisted of different ranks, including lignite, medium and high volatile bituminous. This study considered two lignite samples, named Lig1 and Lig2, and six bituminous samples, termed as Bit1, Bit2, Bit3, Bit4, Bit5, Bit6. Proximate, ultimate, elemental analyses and atomic ratios measured by the Penn State coal sample bank were obtained and analyzed. Table S2 and Fig. S1(a) and (b) present the proximate and ultimate analysis results of all eight coal samples. Both proximate and ultimate analyses show that Lig1 and Lig2 have less carbon content than the bituminous coals. As measured by proximate analysis, the moisture contents of Lig1 and Lig2 samples (33.38 % and 34.91 %, respectively) are much higher than any of the bituminous coals. It is also noted that the oxygen contents of Lig1 and Lig2 are 12.4 % and 10.5 %, respectively, much higher than for the 6-bituminous coal dust samples (4.44 %, 5.17 %, 7.27 %, 6.92 %, 5.18 %, and 4.16 %).

The elemental analysis results, atomic ratios, and reflectance measurements are presented in Table S3 and Fig. S1(c) and (d). The elemental analysis results show a higher carbon, hydrogen and nitrogen content for all six bituminous coal samples than the two lignite coal dust samples, similar to what was observed with proximate and ultimate analysis (Table S2). Also, the two lignites have higher oxygen contents of 17.76 and 15.32 %, respectively, than the six bituminous coal samples measured in elemental analysis. O/C ratios for the two lignite dust samples (0.206 and 0.177, respectively) are higher than all six bituminous coal samples (Fig. S1(d)). This means there are more oxygen atoms per carbon atom in the lignite coal samples than in the bituminous coal samples. Vitrinite reflectance values for all the coal samples are presented in Fig. S1(d). As expected, the reflectance values of the lignite coal samples are much lower than the bituminous coal samples. Reflectance values can represent the degree of coal maturity, with a higher value showing a higher degree of coalification and maturity.

2.2. Preparation of coal dust samples and particle size measurements

Coal samples were pulverized using different crushing methods for EPR analysis. Fig. 1 shows the instruments and step-wised procedure used in the present study.

Each of the eight coal samples was initially hand-crushed by a pestle and mortar to a particle size of <80 mesh (<177 μm), which was suffixed as a hand-crushed (HC) sample. Each HC sample was further pulverized to get respirable coal dust through the cryogenic ball-milling using CryoMill (Retsch Inc.) in the Materials Characterization Lab at Penn State. During the whole cryomill processing, liquid nitrogen was continuously circulated through the autofill system to keep the temperature at −196 °C during milling. Using a liquid nitrogen environment prevents the overheating of the powder sample, which makes the process faster and maintains the original nanopore structure of the coal dust. A maximum of 20 ml of the HC coal dust powders were put into the sample cell. 5 Hz of vibrational frequency was used for pre-cooling, and two cycles with 2 min of each cycle and 30 Hz of vibrational frequency were used. One minute of intermediate cooling time was kept between each cryo-milling cycle. Such coal dust samples were suffixed as Cryomill 2 cycle (Cr2) coal dust samples. Cryo-milling was further performed for four cycles keeping the rest of the cryo-milling parameters the same. Such coal dust samples were suffixed as Cryomill 4 cycle (Cr4) coal dust samples. So, it became three coal dust samples for each, making it a total of 24 coal dust samples used for subsequent analyses. The prepared coal dust samples were kept in an airtight plastic bag and flushed with helium to prevent oxygen adsorption and potential oxidization. It was taken out only during crushing and immediately stored back. During the cooling time in the cryo-milling process, the sample was in a liquid nitrogen atmosphere without oxygen.

The particle size distribution for these samples was measured by Zetasizer Nano ZS located at the Materials Characterization Lab of Penn State. The particle size measurement of the Zetasizer is based on the principle of dynamic light scattering (DLS). The typical measurement range of a Zeta-sizer is 0.3 nm to 10 μm. Before each measurement, each coal dust sample (dispersant) and isopropanol (solvent) were mixed inside a small beaker and put in an ultra-sonic oscillator for about 5 min for preliminary dispersion. A small sample was dispersed in the isopropanol solvent and put in a 12 mm OD (outer diameter) square polystyrene cuvette for aqueous solvents for measurement. It was left undisturbed for 2 min to stabilize the dispersion. Thermally-induced collisions between solvent molecules and the dust particles cause the coal dust particles in the suspension to undergo Brownian motion. As per the principle of DLS, when these randomly moving particles are illuminated with a laser, the intensity of the scattered light fluctuates over time at a rate dependent upon the particle size. Analysis of these intensity fluctuations yields the Brownian motion's velocity and particle size using the Stokes-Einstein relationship. Note that the diameter measured in DLS is called the hydrodynamic diameter and refers to how a particle diffuses within a fluid. Zetasizer software (v8.01) was chosen for data collection and particle size analysis. As shown in Fig. S2, all the prepared coal dust samples contain maximum particles in the respirable range.

2.3. EPR sample preparation and analysis

The characteristics of EPFRs in the 24 prepared coal dust samples were measured using EPR spectroscopy. A measured amount of coal dust sample was put in 4 mm outer diameter EPR tubes (Wilmad labs), properly flooded using helium, and sealed. EPR spectroscopy was performed at X-band using an E-500 ELEXSYS EPR (Bruker Corp.) spectrometer. The measurements were conducted at room temperature in the Super-hi-Q cavity (Bruker BioSpin Corp.) with ESR 900 cryostat (Oxford Instruments). The spectrometer's magnetic field was calibrated using Chromium E1703 Magnetic Field Standard (Magnettech GmbH) with the derivative g value of 1.980. EPR scan parameters were kept the same during all the experiments: modulation frequency, 100 kHz, X-band; microwave frequency, about 9.87 GHz; attenuation, 40 dB; time constant-50 ms and number of scanning points-2048. All the observations were accomplished in the air at ambient temperature

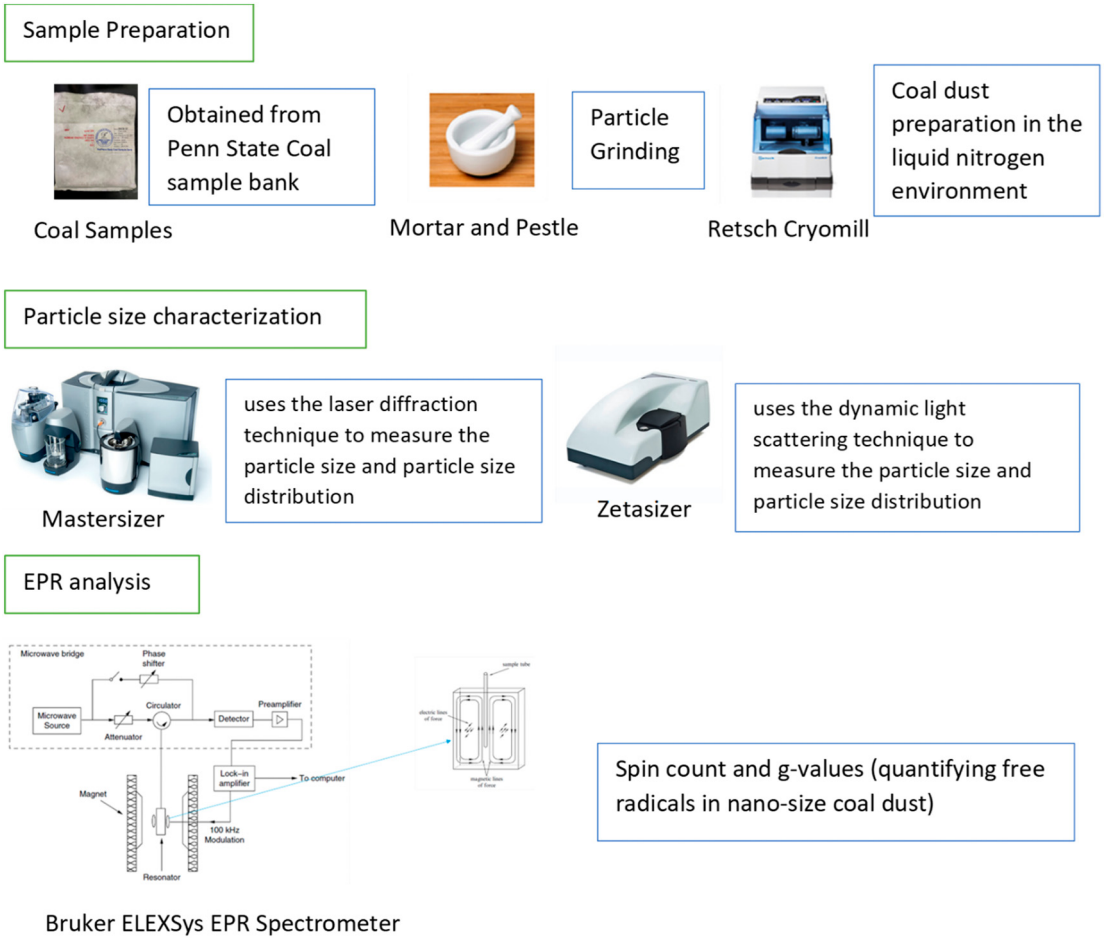

Fig. 1. Coal dust sample preparation, particle size analysis and EPR analysis of coal dust samples. (Modified from R. Zhang et al. (2021).)

and atmospheric pressure. EPR scans were performed with the Bruker computer software WinEPR Acquisition. The parameters recorded and further calculated from EPR spectra are *g*-value and spin concentration (radical intensity, i.e., concentrations of paramagnetic centers). The intensity of the signal was obtained by double integration of the signal. To determine the number of spins in the sample, a series of 4-hydroxy-TMPO free radical samples with a known number of spins was measured, and a calibration curve was plotted (see supplement Fig. S3). To ensure that all spins in the samples were accounted for, the sample length was 25.4 mm, which kept the whole sample in the resonator. For comparison purposes, the total number of spins (μmol) was normalized by weight by dividing the calculated spin count by the weight of the sample.

2.4. Correlation analyses

One of the primary purposes of this study was to understand the characteristics of coal dust, which determines the nature and content of coal dust. Proximate, Ultimate, Elemental analysis, O/C and reflectance are some preliminary tests performed to understand the nature of coal. Most of the time, these tests are sufficient to provide enough information about the type and nature of coal. Hence, the goal was to see if the same primary tests done for coal could help provide some information about the free radical content of coal dust. Through correlation analysis, we found the possible characteristics of coal dust which could play a major role in determining the type and nature of free radicals. We found that carbon and oxygen are the main content of coal dust which play a prominent role in deciding EPFR characteristics. Also, we know that carbon is the main content of coal dust, so its role in affecting the EPFR characteristics was extremely important to understand. Hence, we mainly separated the correlation analysis of carbon and EPFR g-values and spin counts. We know that several statistics, such as p-value, residual r-square, and r-square, found through fitting analysis, are mathematical indicators and evidence of strong correlation. Hence, they were performed and mildly discussed to the point to make our objectives more understandable. It is expected that the correlation performed in the present analysis could be reasonably used to assess the future EPFR-modulated toxicity of coal dust.

Correlation analysis was performed between the proximate, ultimate, and elemental analysis, atomic ratios and reflectance measurements and the spin counts and g-values obtained by the EPR spectroscopy. A correlation was performed to find relationships between the coal characteristics (indicators) and EPR values (spin counts and *g*-values) which are the indicators of the toxicity of coal dust. The Pearson correlation coefficient between the coal dust characteristics and the EPR calculated values was calculated. The Pearson correlation coefficient between two random variables, X and Y, measures their linear dependence. The Pearson correlation ($\rho(X, Y)$) is defined as:

$$\rho(X,Y) = \frac{1}{N-1}\sum_{i=1}^{N}\frac{(X_i-\mu_X)}{\sigma_X}\frac{(Y_i-\mu_Y)}{\sigma_Y} \quad (1)$$

where N is the number of observations, μ_X and σ_X are the mean and standard deviation of variable X, and μ_Y and σ_Y are the mean and standard deviation of variable Y. The correlation coefficient matrix of two random

variables is the matrix of correlation coefficients for each pairwise variable combination as:

$$M = \begin{pmatrix} \rho(X,X) & \rho(X,Y) & \dots \\ \rho(Y,X) & \rho(Y,Y) & \dots \\ \vdots & \vdots & \ddots \end{pmatrix} \quad (2)$$

The correlation coefficient is a scalar value in the (−1,1) range. A correlation coefficient value close to 1 implies a positive correlation, whereas a value of −1 implies a negative correlation between two variables. p-Values were also calculated for the correlation between the two variables using the Pearson correlation coefficients using t-distribution given by:

$$t = \frac{\rho\sqrt{N-2}}{\sqrt{1-\rho^2}} \quad (3)$$

where ρ is the Pearson correlation coefficient between two variables and N is the number of observations. p-Values range from 0 to 1. A small p-value is an indication that the null hypothesis is false. It means that the correlation coefficient differs from zero and a linear relationship exists.

The linear regression analysis was done to understand the relation between the scalar response (EPR spin counts and *g*-values) and the explanatory variables (coal dust characteristics). The form of linear equation used is:

$$y = a + bx \quad (4)$$

where y is the dependent variable (EPR spin counts and *g*-values) and x is the independent variable (coal dust characteristics). a and b are the intercept and slope of the fitted lines. The residual sum of squares (RSS) is calculated from the linear fit using:

$$RSS = \Sigma_{i=1}^{n}(y_i - f(x_i))^2 \quad (5)$$

where y_i is the ith value of the variable to be predicted, x_i is the ith value of the explanatory variable, and $f(x_i)$ is the predicted value of y_i. The smaller the residual sum of squares, the better the model fits the data. Coefficient of Determination (COD) or R^2 which means the percentage of the response variable variation explained by the fitted regression line is also calculated. COD is given by:

$$R^2 = 1 - \frac{SS_{Res}}{SS_{Tot}} \quad (6)$$

SS_{Res} and SS_{Tot} are the sum of squares of residuals and the total sum of squares, respectively, given by:

$$SS_{Res} = \Sigma_{i=1}^{n}(y_i - f(x_i))^2 \quad (7)$$

$$SS_{Tot} = \Sigma_{i=1}^{n}(y_i - \bar{y})^2 \quad (8)$$

where $\bar{y}$ is the mean of the observed data. R^2 is always between 0 and 1. R^2 value of 1 indicates that the fitted line explains all the variability of the response data around its mean. In general, the larger the R^2, the better the fitted line fits the data. The adj. R^2 is also calculated for the linear fit. The Adj. R^2 is a modified version of the R-square, adjusted for the number of predictors in the fitted line. Its mathematical expression is in the form of the following:

$$R^2_{adj} = \frac{(1-R^2)(N-1)}{(N-P-1)} \quad (9)$$

P is the number of predictors and R^2 is the COD. The values of the Linear fit analysis and corresponding R^2, RSS, R^2_{adj} and Pearson's r values are put in a box inside the corresponding graphs, wherever they are plotted.

3. Results

This study aimed to understand the characteristics of the EPFRs present in different types and ranks of coal and how these characteristics correlate with the properties of coal obtained through different analysis methods. The EPR measurements of all 24 samples were taken on three different days, i.e., 24th December 2021, 28th February 2022 and 28th April 2022. These EPR measurements are shown in Figs. S4, S5 and S6. By comparing EPR curves collected on different days, all the absorption lines appear similar, i.e., symmetric curves without hyperfine structures. However, the intensities and locations are distinguished from each other. Typically, EPR spectra of pure materials such as methyl display hyperfine structures associated with hyperfine splitting. However, coal is a complex structure with multiple paramagnetic centers and usually shows smooth curves without hyperfine splitting (Zhou et al., 2019). The peak area of the EPR spectra is used to obtain the concentration of EPFRs, and Lande *g*-values depend upon the peak position. The *g*-values are unique in that they are regarded as the material's fingerprint. This means that the *g*-values of coal dust samples reflect the combined feature of all the types of radicals within them because of their chemically heterogeneous nature (Liu et al., 2014). The Lande *g*-value is the ratio of the electron's magnetic moment to its angular momentum. It is calculated using the relationship:

$$g = \frac{h\nu}{\mu_B B_r} \quad (10)$$

In Eq. (10), g is the Lande g-value, h is the Planck's constant (6.626176×10^{-34} joule-seconds), ν is the microwave frequency (9.87 GHz), μ_B is the Bohr magneton (9.274×10^{-24} J·T^{-1}), and B_r is the magnetic field strength. EPR spin counts (μmol/g) and g-values were calculated from the raw data (Table S4). Fig. 2(a), (b) and (c) shows the concentration of EPFRs (spin counts, μmol/g) calculated for Hand Crushed, Cryo 2 and Cryo 4 samples, respectively. It was noted that the spin counts, as calculated from the EPR data, remained constant, and there was an insignificant change for all three measurement days (Fig. 2). This suggests that the free radicals in the coal dust are persistent in nature and can stay stable for months. Hence, these free radicals are persistent and should be termed as EPFRs. Average values and standard deviations of the spin counts and the *g*-values are also shown in Table S4. Generally, the *g*-values of the coal dust particles are higher than that of free electrons ($g_E = 2.0023$) due to the spin-orbit coupling of EPFRs and also interactions with native atoms and lattice in the coal dust (Liu et al., 2014).

Based on the tested coal samples, the *g*-values were distributed between 2.0029 and 2.0037 (Table S4). Note that the *g*-values indicate the nature of the paramagnetic species and are unique for an unpaired electron in a typical environment. This means that an unpaired electron has a unique *g*-value in a given chemical environment. The *g*-values in the range of 2.003 to 2.0037 are characteristics of oxygenated carbon-centered or a mixture of oxygen or carbon-centered EPFRs, in which case the free electron can get delocalized over oxygen (Liu et al., 2014; Petrakis and Grandy, 1978; Xu et al., 2019). It can be seen in Tables S2 and S3 that the bituminous coal has less oxygen content than the lignite coals corresponding that they have lower *g*-values. This suggests that the EPFRs in the bituminous coal dust are mainly oxygenated carbon-centered free radicals. Whereas the lignite coals have higher oxygen contents and fewer carbon contents, meaning more oxygen around the EPFRs in them, and hence their *g*-values are close to 2.0037. It is well known that the EPR spectra of coal are smooth because it has multiple paramagnetic species (Zhou et al., 2019). Also, several studies have documented that a larger *g*-value of coal means the presence of more heteroatom-containing radicals due to their stronger spin-orbit coupling interactions (Zhou et al., 2019). Based on this, it can be thought that the free radicals in lignite can be oxygenated carbon centered or maybe a mixture of carbon and oxygen-centered free radicals.

Another observation from Table S4 is that all the bituminous coal dust samples have several orders of magnitude higher EPFR concentrations

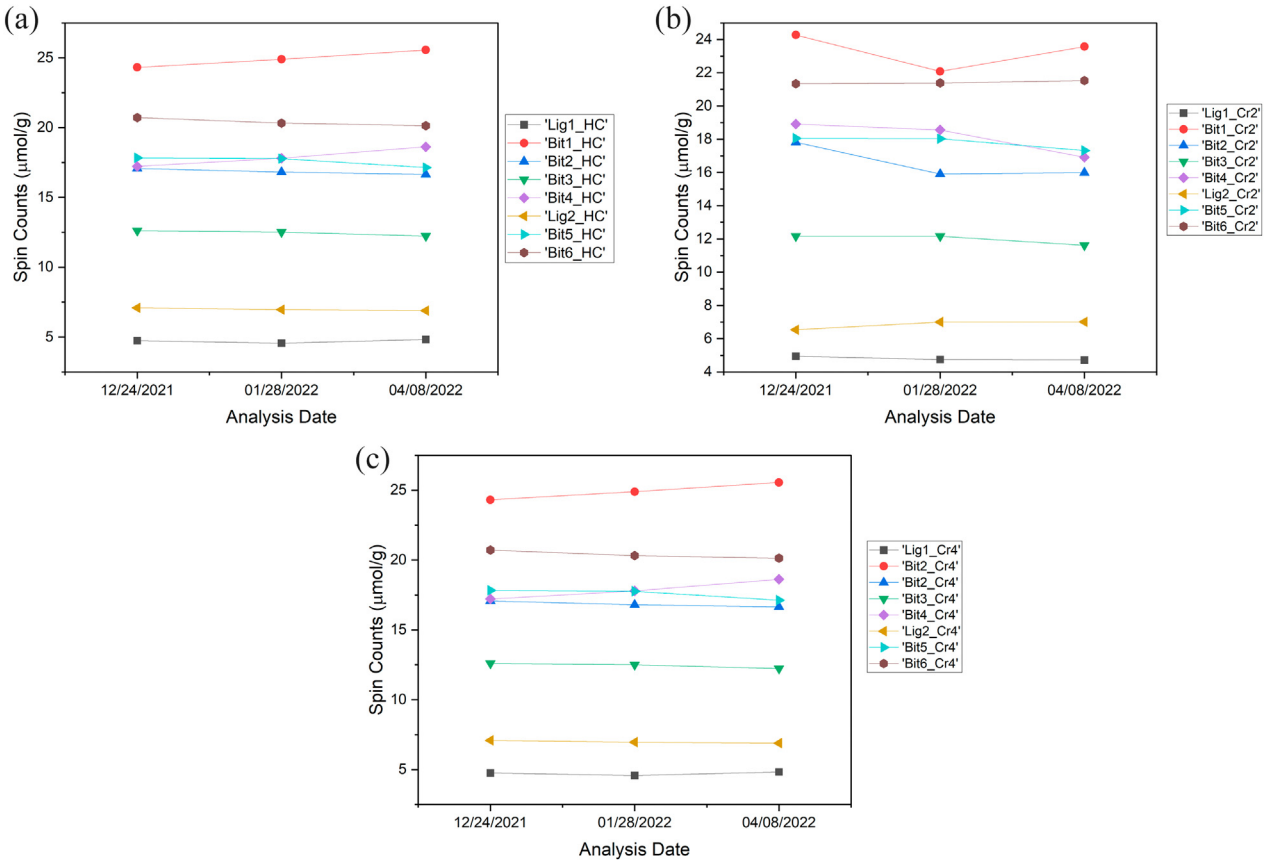

Fig. 2. Spin counts calculated from EPR analysis of different coal dust samples: (a) Spin counts for hand crushed coal dust samples; (b) spin counts for cryo-milled two cycles coal dust samples; (c) spin counts for cryo-milled four cycles coal dust samples.

than the lignite coal dust. Several other studies have noted similar results (Petrakis and Grandy, 1978; Pilawa and Więckowski, 2007). The stability of free radicals in coal originates from the metamorphism of organic coal substances in geological time. Bituminous coal has gone more metamorphism than lignite coal meaning bituminous coal was created after surviving at high pressure and temperature for a long extended period (Pilawa and Więckowski, 2007). Hence, their paramagnetic centers are even resistant to difficult paleo-environmental conditions, and more paramagnetic centers can be produced from bituminous coal than lignite coal. This work presented a correlational study to determine the correlation between coal dust characteristics correlated with EPFR values and their possible implications on health risk potential.

3.1. Correlation between EPFRs characteristics and the proximate analysis of coal dust

Proximate analysis of the prepared coal dust is a simple means of determining the distribution of products obtained when the coal sample is heated under specified conditions. It provides an assay of the (1) *moisture*, (2) *volatile matter*: consisting of gases and vapors driven off during pyrolysis, (3) *ash*: the inorganic residue remaining after combustion and (4) *fixed carbon*: the non-volatile fraction of coal ("Proximate Analysis," 2015). Fig. 3 shows the relationships between the EPR calculated values and the coal dust proximate analysis values for all prepared coal dust. We have already discussed that based on the *g*-values, the free radicals are oxygenated carbon-centered in the coal dust in the present analysis. From Fig. 3, it is apparent that the EPFR g-values and spin counts are positively correlated with the moisture and fixed carbon content of the coal dust.

Lignite coal dust has a higher moisture content than the bituminous coal dust samples (Fig. S1(a)); correspondingly, they have higher g-values and lower spin counts. As discussed above, the higher *g*-values in the lignite (>2.0035) show that the free radicals in the lignite coal dust are either oxygenated carbon centered or a mixture of both carbon and oxygen-centered free radicals.

Similarly, we see a strong correlation between the EPFRs spin counts and *g*-values and the fixed carbon content of the coal dust. Bituminous coal has higher fixed carbon content, smaller *g*-values, and higher spin counts. Similar observations have been made in earlier studies, and some have found that the *g*-values decrease with the increase in coal maturity (Liu et al., 2014). As mentioned, bituminous coal has matured more; hence, the coal dust produced from the lignite coals has lower carbon contents. There is no significant correlation between the ash and volatile content of the coal dust and the EPFR concentration and *g*-values (Fig. 3). The Pearson correlation matrices are listed in Table S5. Table S5 asserts the visual observation that there is a strong linear dependence between the fixed carbon content and the EPFR spin counts and *g*-values. The *g*-values confirm that the free radicals are oxygenated carbon-centered for bituminous coal dust. Increasing spin counts means that with increased carbon content in the tested coal dust, the concentration of EPFRs increases. p-Values for the linear combination of coal dust EPFR characteristics and the fixed carbon content are extremely small (Table S5). This again suggests a strong linear relationship between the EPFR characteristics and the fixed carbon content.

Another key point is that the increase in moisture content decreases the carbon content of the coal. The two lignite coals have several times higher moisture content when compared to the six bituminous coal samples, as shown in Table S2, and consequently, they have a much lower carbon content. Hence, a strong negative correlation was observed between the moisture content and the EPFR spin count, along with a positive correlation between the moisture content and EPFR *g*-values (Table S5).

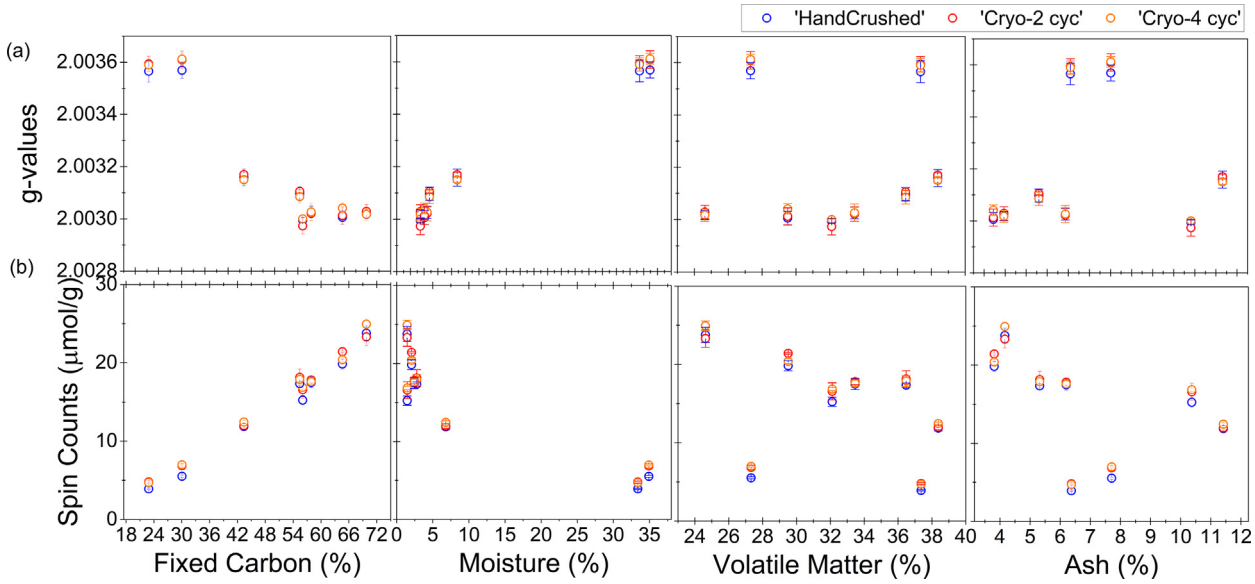

Fig. 3. Average of (a) g-values and (b) spin counts; calculated using EPR for hand-crushed, Cryomill-2 cycles and Cryomill-4 cycles coal dust samples plotted against their proximate analysis values – Fixed carbon (%), moisture (%), volatile matter (%), ash (%). A strong correlation between the average g-values/spin-counts and the carbon (%) can be observed. Error bars shows the standard deviation for the spin counts and g-values.

Noticeably, there is a strong correlation between the EPFR characteristics and the fixed carbon content of the coal dust. A linear fit analysis was done between them, as shown in Fig. 4. The linear fit model and the corresponding fit analyses between the scalar response (EPFR spin counts and *g*-values) and the explanatory variables (fixed carbon) are mentioned in the inner boxes in the graphs (Fig. 4(a) & (b)). The dotted lines show the plot of the linear fitting line, and the fitting parameters are listed on each figure. EPFR characteristics (*g*-value and spin counts) correlate well to the fixed carbon content of coal dust. Pearson's *r* value is close to the -1, meaning a strong negative correlation exists between the EPFRs *g*-values and the fixed carbon content of coal dust. R^2, R^2_{adj} and RSS are reasonably good for the linear fit between the EPFR *g*-value and fixed carbon content (box of Fig. 4(a)). Similarly, the linear fit excellently predicts the calculated values of the EPFR spin count with the fixed carbon content of coal dust (box of Fig. 4(b)). R^2, R^2_{adj} are extremely close to 1, showing an excellent linear fit (box of Fig. 4(b)).

Overall, it was observed that the EPFRs in the coal dust samples correlate well with the fixed carbon content of the coal. An increase in the carbon content of coal could suggest an increase in the EPFR concentration of the coal dust.

3.2. Correlation between EPFR characteristics and ultimate/elemental analyses of coal dust

This section discusses the correlations between the EPFR characteristics and ultimate and elemental analysis results. Ultimate analysis of coal dust is

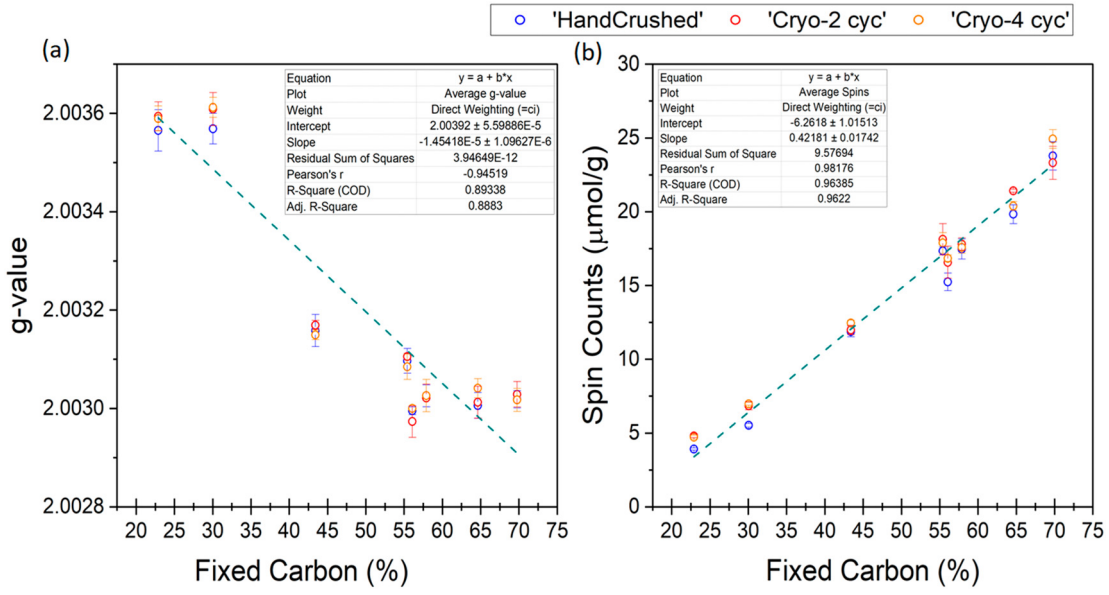

Fig. 4. Linear fit between (a) g-values and fixed carbon (%); (b) spin counts and fixed carbon (%); from proximate analysis. The boxes inside both (a) and (b) shows the calculated linear fit parameters. Error bars shows the standard deviation for the spin counts and g-values.

used to determine the carbon, hydrogen, nitrogen, sulfur and ash contents of the coal. The carbon (%) measured in the ultimate analysis is the carbon present as organic carbon occurring in the coal material and carbon present as mineral carbonate. Hydrogen (%) is the total hydrogen present in the organic material of the coal as well as the hydrogen associated with the water in the coal. Nitrogen (%) is assumed to be the sum of nitrogen in the organic matrix of the coal. Sulfur (%) measured in the ultimate analysis is the sum of sulfur present in the organic sulfur compounds, inorganic sulfur, that is mainly in the form of iron sulfides, pyrites and marcasite and also inorganic sulfates such as (Na_2SO_4, $CaSO_4$). Similarly, elemental analysis of coal provides information about carbon, oxygen, nitrogen, hydrogen, mineral matter, and organic sulfur content in the coal.

Figs. 5 and 6 are the plots of EPFRs characteristics (spin counts and g-values) of the prepared coal dust with their ultimate and elemental analyses, respectively. As expected, a good correlation exists between the *g*-values and spin counts of EPFR and total carbon content (%). As shown in Figs. 5(a) and 6(a), the g-value is inversely proportional to the carbon content of the coal increases. In contrast, Figs. 5(b) and 6 (b) show that spin count is proportional to the carbon content of the coal. It should be noted that the fixed carbon measured in the proximate analysis is measured as a difference of the material remaining after determining moisture, volatile matter, and ash. Some carbon is lost in hydrocarbons with the volatile matter during proximate analysis. Whereas, as already mentioned, the carbon determination in the ultimate analysis of coal includes carbon present as organic carbon and carbon present as mineral carbonate. Considering that, fixed carbon content is the major determinant of free radical characteristics in coal dust.

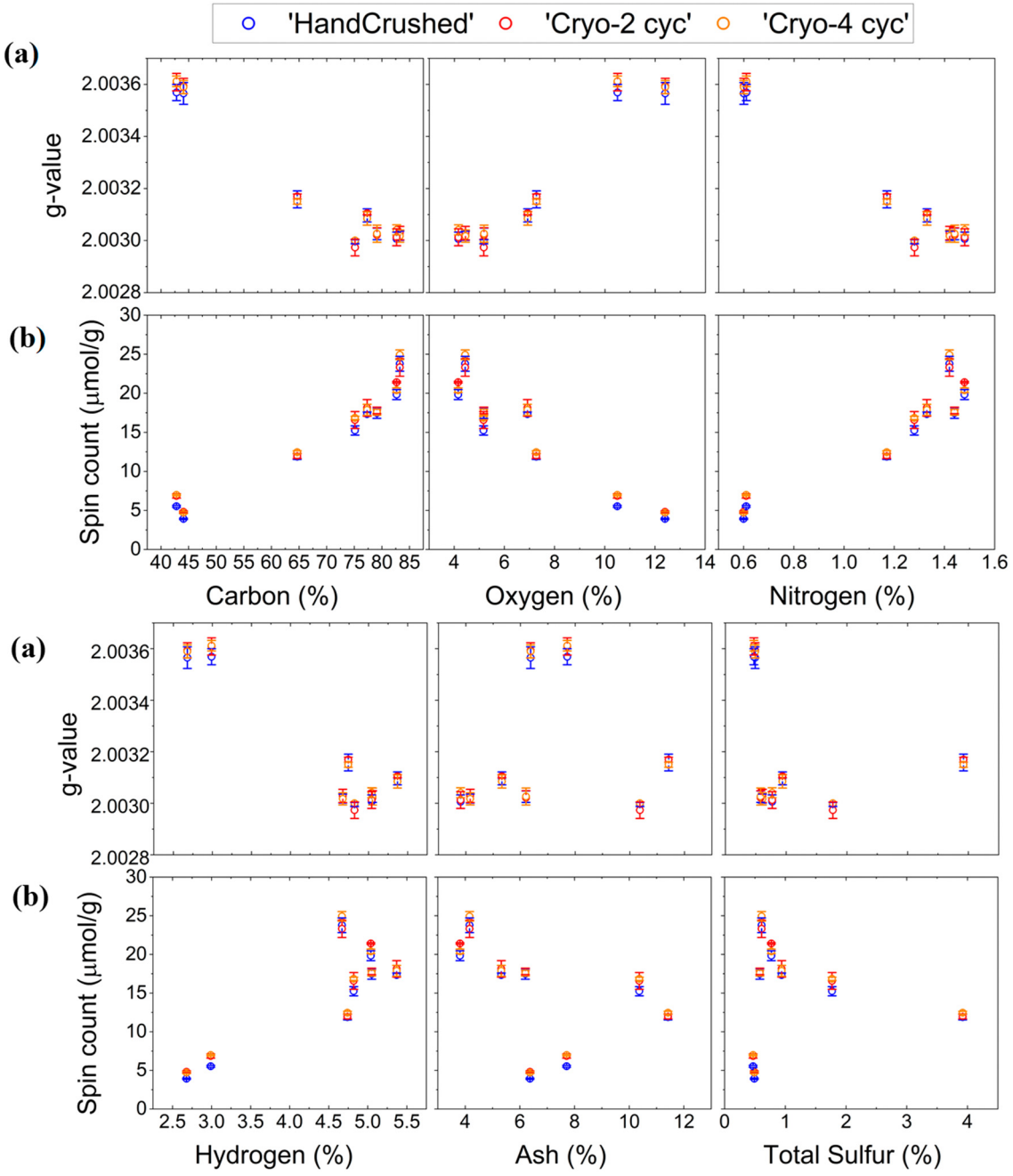

Fig. 5. Average of (a) g-values and (b) spin counts; calculated using EPR for hand-crushed, Cryomill-2 cycles and Cryomill-4 cycles coal dust samples plotted against their ultimate analysis values – carbon (%), oxygen (%), nitrogen (%), hydrogen (%), Ash (%), total sulfur (%). A strong correlation between the average g-values/spin-counts and the carbon (%) can be observed. Error bars shows the standard deviation for the spin counts and g-values.

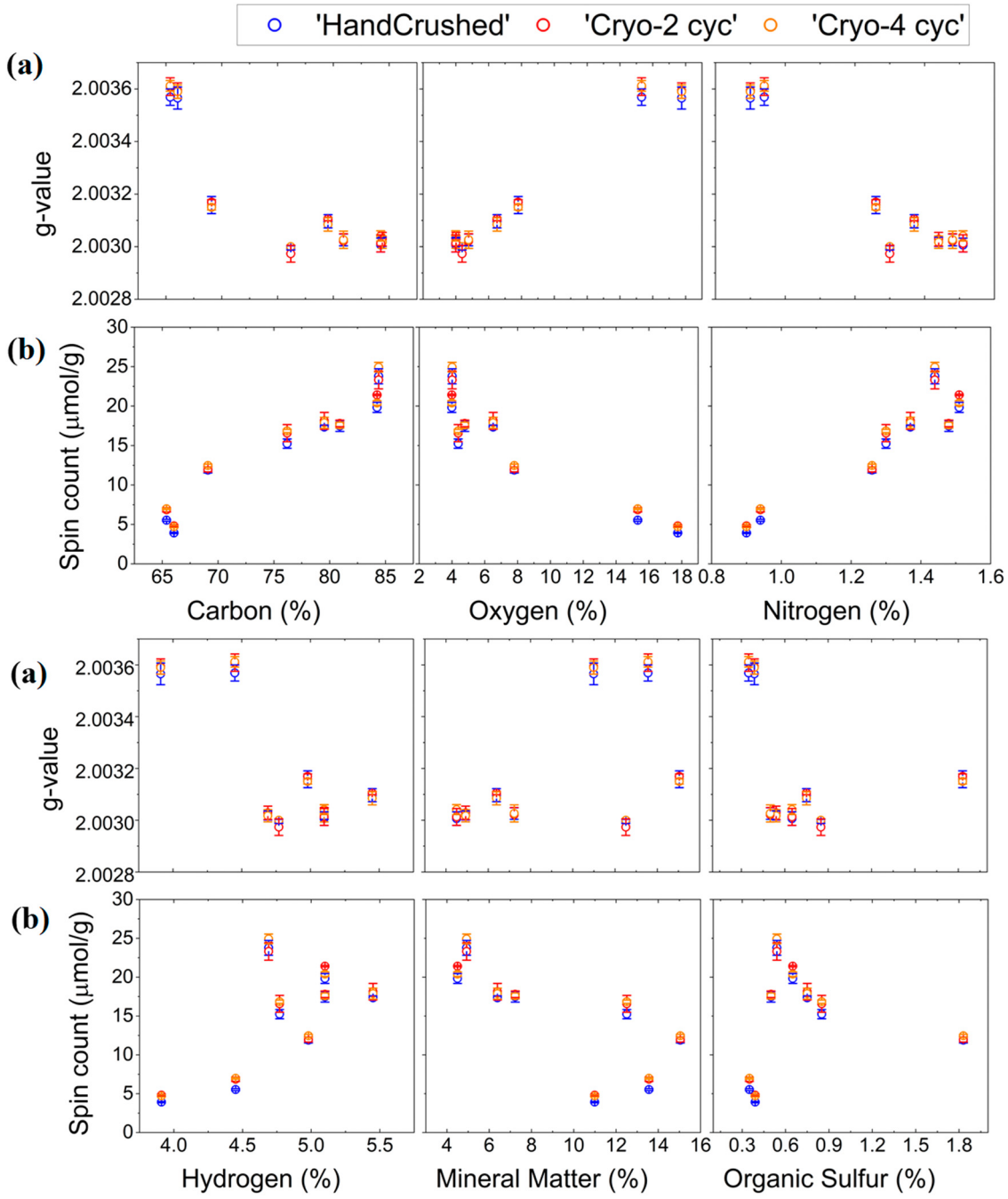

Fig. 6. Average of (a) g-values and (b) spin counts; calculated using EPR for hand-crushed, Cryomill-2 cycles and Cryomill-4 cycles coal dust samples plotted against their elemental analysis values – carbon (%), oxygen (%), nitrogen (%), hydrogen (%), mineral matter (%), organic sulfur (%). A strong correlation between the average g-values/spin-counts and the carbon (%) can be observed. Error bars shows the standard deviation for the spin counts and g-values.

An extremely small p-value for the correlation between carbon and *g*-values and spin counts of EPFR and carbon (%) suggests a strong linear relationship (Tables S6 and S7). The *g*-value correlates negatively with the carbon (%) in both cases (Tables S6 and S7). These observations are similar to the observations in the case of proximate analysis (see Fig. 3). All of the bituminous coal dust have carbon concentrations of >60 %, whether from the ultimate elemental analysis (see Tables S2 and S3); hence they have lesser *g*-values and higher spin counts (see Table S4). Overall, it is observed that the chemical environment (represented by *g*-value) of EPFRs is representative of the coal dust characteristics and that more carbon in the coal dust leads to a more stabilized free radical concentration. It can also be seen that there is a good linear dependence between the *g*-value of EPFR and oxygen (%) for both ultimate and elemental analysis (see p-values in Tables S6 and S7). Specifically, Tables S6 and S7 mean a positive correlation exists between the g-value of EPFR and oxygen (%) for both ultimate and elemental analyses, meaning the *g*-values increase as the oxygen content in the coal dust increases. Lignite coal has a higher oxygen concentration than bituminous coal (Tables S2 and S3).

As discussed earlier, as the EPFR can localize more and more on the oxygen atoms, the measured *g*-values increase. The negative correlation between the spin counts and oxygen (%) for both ultimate and elemental analysis (see Tables S6 and S7) is attributed to the higher coal maturation, which has more stabilized free radicals associated with lower oxygen content, i.e., bituminous coal. A similar positive correlation was observed between the moisture content and *g*-values of the coal dust (see Table S5). Moisture (H_2O) also has oxygen and hydrogen in

its molecular structure. However, the hydrogen is not strongly correlated with the EPFR *g*-values. The oxygen content is closely related to *g*-values, as shown in Tables S6 and S7. This means that the oxygen content of coal dust correlates with the absolute amount of oxygen in the coal dust, whether inherited or present in the form of moisture. Nitrogen (%) is also measured as a part of the ultimate and elemental analysis of coal. It is noted that there is a good linear dependence between the *g*-value of Carbon-Centered EPFR (CCEPR) and nitrogen (%) for both ultimate and elemental analysis (see p-values in Tables S6 and S7). Moreover, there is a negative correlation between the *g*-values of CCEPFRs and nitrogen (%) (Tables S6 and S7). Earlier studies have reported that the nitrogen-containing CCEPFRs have similar *g*-values as those containing oxygen. Hence, it has been found that the nitrogen-containing CCEPFRs have a *g*-value close to 2.0031 (Liu et al., 2014; Petrakis and Grandy, 1978). Tables S2 and S3 mention that the nitrogen (%) of bituminous coal is always higher than that of lignite coal. Consequently, we see that all the bituminous coal dust has a *g*-values closer to 2.0031 when compared to the lignite coal dust.

A strong linear dependence was not observed between CCEPFR characteristics, ash (%), total sulfur (%) from the ultimate analysis and organic sulfur (%) from the elemental analysis of the coal (see Tables S5 and S6). Similarly, a weak correlation is observed between the CCEPFR characteristics and mineral matter (%) from elemental analysis. It should be noted that mineral matter in coal is an inclusive term that refers to the mineralogical phases and all other inorganic elements in coal. Inorganic elements in coal include elements that are bonded in various ways to the organic (C, H, O, N, S) components (Speight, 2015). Some of these elements may correlate with the EPFR characteristics of the coal dust; however, that study is a part of planned work to be accomplished in the future.

A linear fit analysis was also done between the CCEPFR characteristics and carbon (%) from ultimate and elemental analysis. Linear fit plots, along with the calculated values, are shown in Figs. 7 and 8. The inner boxes in these figures show the linear fitting statistics for the corresponding fit. The g-values predicted by the linear fit are close to the measured values. Overall, Pearson's *r* for the linear fit between CCEPFR values and ultimate and elemental analysis carbon (%) is −0.98013 and −0.89958 (close to −1), respectively, showing a negative and good correlation (see inner boxes of Figs. 7(a) and 8(a)). The R^2 values are 0.9606 and 0.8095, and *adj*.R^2 values are 0.95879, and 0.80017 for ultimate and elemental analysis carbon (%), respectively, meaning that a large percentage of the variable response variation explained is well explained by the fitted regression line. Similar observations can be made for the CCEPFRs spin counts and carbon (%) from ultimate and elemental analysis (Figs. 7(b) and 8(b)). It can be seen that for the positive correlation between CCEPFRs spin counts and carbon (%), Pearson's *r* is positive (0.92673 and 0.94889, respectively). The R^2 and *adj* R^2 are >0.85 (close to 1), showing the linear fit was able to predict values of spin counts close to those measured using EPR spectroscopy.

3.3. Correlation between EPR values and the atomic ratios and reflectance of coal dust samples

This section will discuss the correlation between the EPFRs characteristics and the atomic ratios and reflectance of coal. The atomic ratios of different types of atoms in coal provide information about its structure. In fact, atomic ratios have played a key role in determining coal molecular structure throughout the literature (Mathews and Chaffee, 2012). The reflectance of coal can be used as an indicator of the maturity of the coal in the hydrocarbon source rocks (Speight, 2015). Usually, the reflectance of coal increases with the increase in maturity. Fig. 9(a) demonstrates the CCEPFR g-values, and spin counts plotted against the H/C, O/C and reflectance of coal dust. No obvious correlation was observed between the CCEPFRs characteristics and the H/C ratio of the coal dust (Fig. 9(a)). The correlation coefficient between CCEPFRS characteristics and H/C ratios is close to zero (Table S8), and p-values are also considerably higher (Table S8), meaning almost no correlation. However, we see a good correlation between the O/C ratio and the CCEPFRs g-values and spin counts (Fig. 9). The correlation coefficients are close to 1 (Table S8), and the p-values extremely small (Table S8). The g-values of the EPFRs in the coal dust are directly proportional to their O/C values. The reason for such a correlation is that increasing O/C ratios mean that more and more oxygen (heteroatom) atoms are coming around EPFRs on which electrons can be delocalized, leading to an increase in the g-values. It can also be seen from elemental (Table S3) and ultimate analysis (Table S2) that the increase in O/C ratios is accompanied by a decrease in carbon (%) and an increase in oxygen (%). This means the lignite coal dust has higher oxygen, lower carbon content, and a high O/C ratio (see Table S3). It has already been discussed that lignite coal dust has higher g-values than bituminous coal dust. Correspondingly, there is a decrease in the spin counts with an increase in the O/C ratios (Fig. 9(b)). This corroborates with the low spin counts observed for lignite coal dust in the previous sections.

A good correlation between the EPFRs characteristics and reflectance is also observed, as shown in Fig. 9(a) and (b). As discussed above, the reflectance indicates the maturity of the coal, and a higher reflectance implies more maturity. The coal which has undergone a higher degree of coalification (more mature) will have a higher degree of aromatic structures, as these structures are extra stable because of their resonance and conjugation

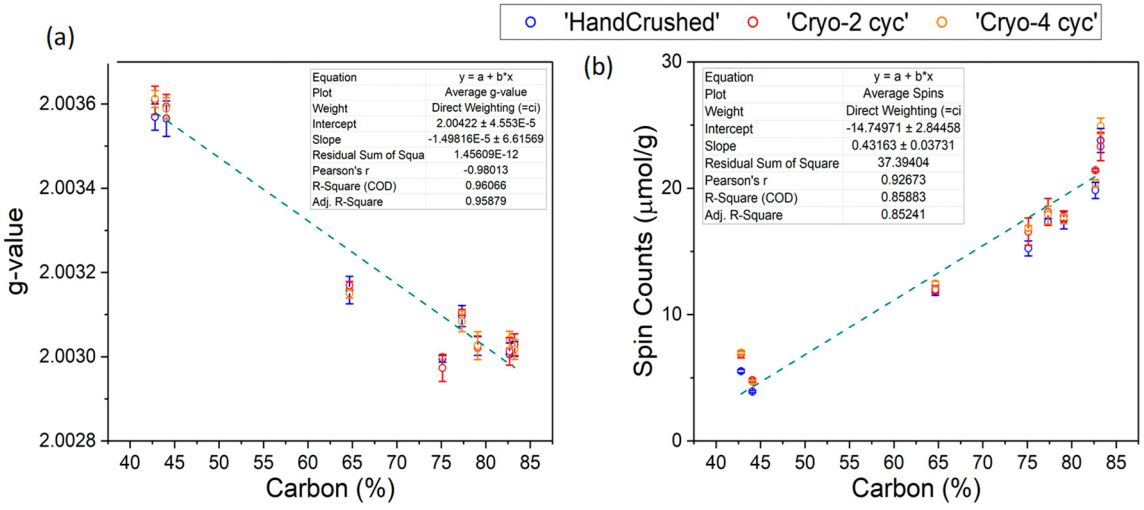

Fig. 7. Linear fit between (a) g-values and carbon (%); (b) spin counts and carbon (%); from ultimate analysis. The boxes inside both (a) and (b) shows the calculated linear fit parameters. Error bars shows the standard deviation for the spin counts and g-values.

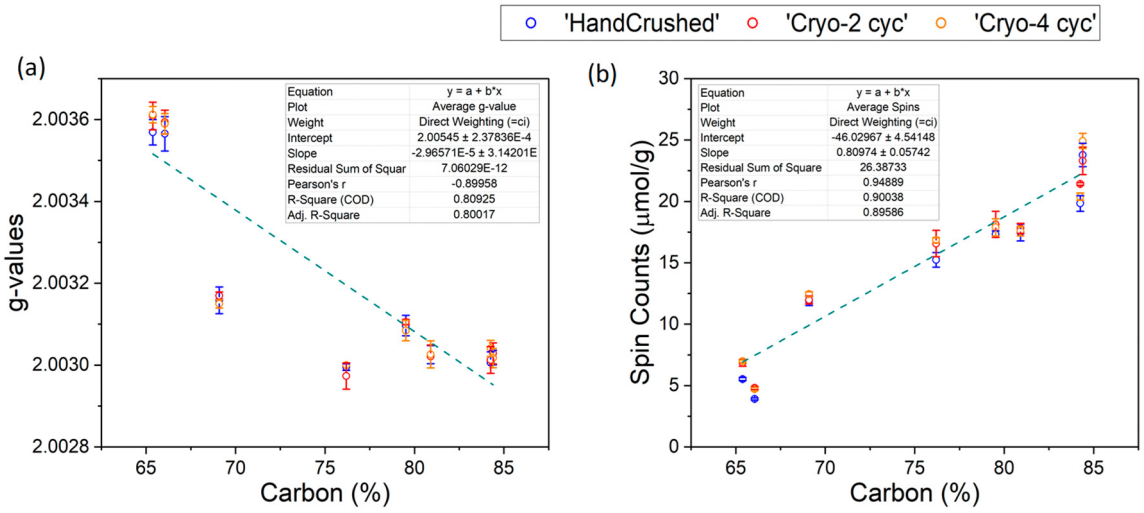

Fig. 8. Linear fit between (a) g-values and carbon (%); (b) spin counts and carbon (%); from elemental analysis. The boxes inside both (a) and (b) shows the calculated linear fit parameters. Error bars shows the standard deviation for the spin counts and g-values.

characteristics. Hence, they can possess more quantity of stable free radicals. Such as bituminous coal has undergone longer and more intense coalification than lignite coal; hence, they are more mature. The coal, which has undergone more maturity, usually has higher carbon content and lower heteroatoms or other metal or trace elements. This is why we see that as the maturity increases, the g-values decrease, and there is a negative correlation between the EPFR g-value and the reflectance (Fig. 9(a), Table S8). Furthermore, there is a positive correlation between the spin counts of EPFRs and the reflectance of coal dust (Fig. 9(b)). This means that more mature coal has a higher number of EPFRs. This is because of the great stability of paramagnetic centers in the atomic structures of more matured coal, which comes from the metamorphism of organic coal substance at the geological time scale (Pilawa and Więckowski, 2007).

A linear fit analysis was performed between the CCEPFR characteristics of coal dust and the O/C ratio and reflectance, shown in Fig. 10. Fig. 10(a) and (b) shows that the values predicted by the linear fit equation for fit between g-value/spin counts and O/C are well correlated with the experimental values with a Pearson's r value of 0.98431 and − 0.86588, respectively. The R^2 and *adj* R^2 values between the linear fit and experimental values for the CCEPFRs g-values and O/C are also close to 1, and *RSS* is extremely small, meaning that a large percentage of the response variable variation explained is well explained by the fitted regression line. The R^2 and *adj* R^2 for spin counts vs. O/C ratios are relatively lower, and *RSS* is also slightly higher, meaning a lesser consistency between the predicted and experimental values using a linear fit equation (Fig. 10(b)). The linear fit analysis between the CCEPFR

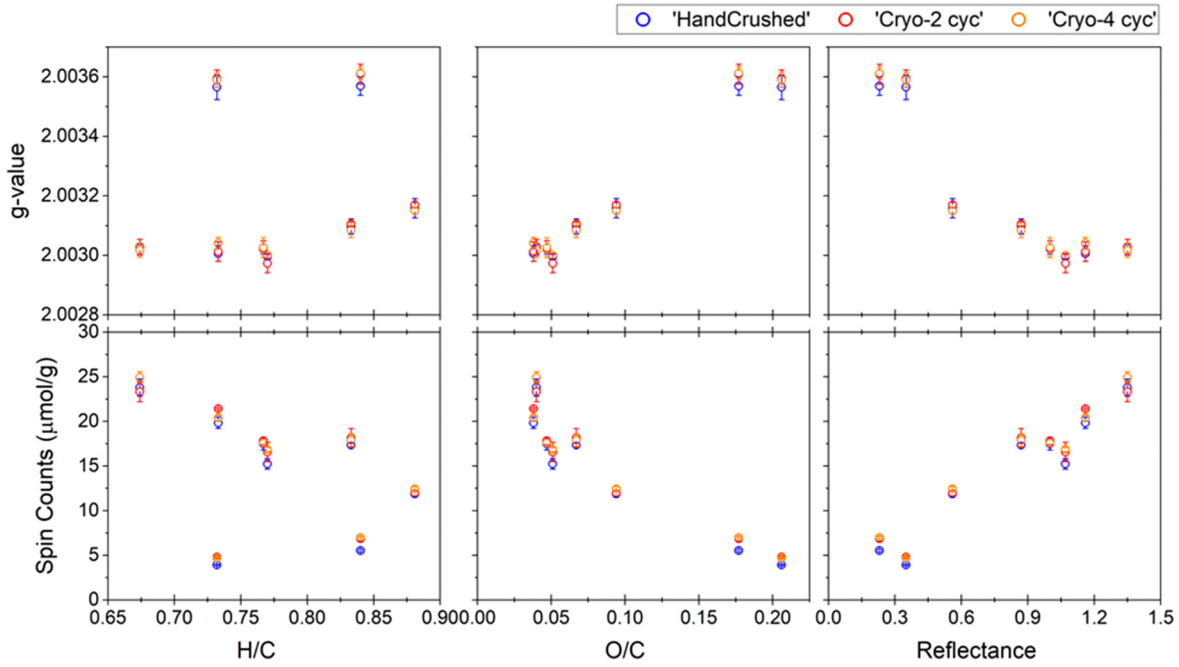

Fig. 9. Average of (a) g-values and (b) spin counts; calculated using EPR for hand-crushed, Cryomill-2 cycles and Cryomill-4 cycles coal dust samples plotted against their atomic ratios – H/C and O/C, and reflectance. Error bars shows the standard deviation for the spin counts and g-values.

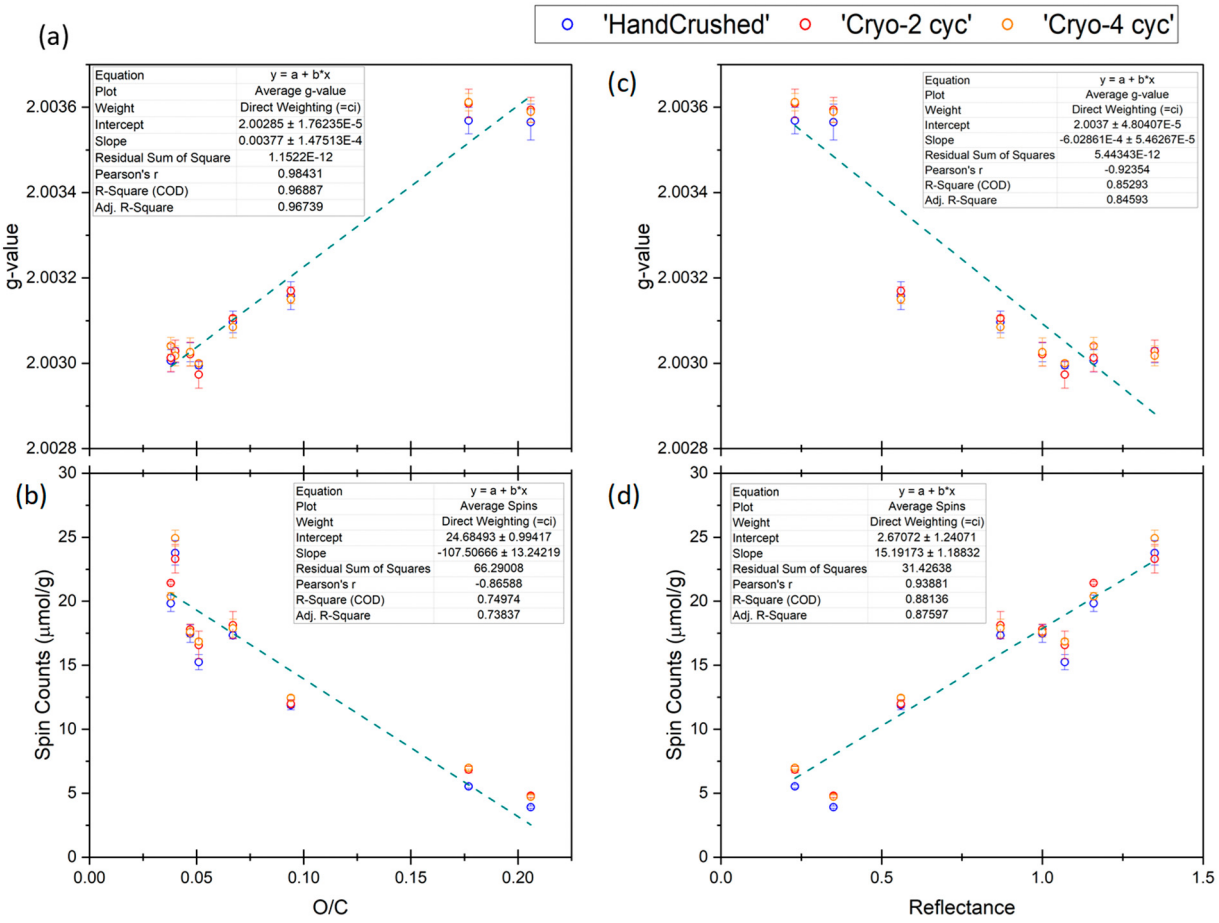

Fig. 10. Linear fit between (a) g-values and O/C ratio; (b) spin counts and O/C ratio; (c) g-values and reflectance; (b) spin counts and reflectance. The boxes inside both (a), (b), (c) and (d) shows the calculated linear fit parameters. Error bars shows the standard deviation for the spin counts and g-values.

characteristics of coal dust and the reflectance also shows a good correlation between the fit and experimental values with a Pearson's *r* value of −0.92354 and 0.93881, respectively (Fig. 10(c) and (d)). Both R^2 and *adj* R^2 values for the linear fit between g-values and spin counts are >0.84, showing that the fitted line reasonably explains all the variability of the response data around its mean.

4. Discussion

EPFRs have been identified as a new class of environmental pollutants. Several studies have observed the role of EPFRs in the particulates affecting their toxic properties. One of the most important ways the particulate-bound EPFRs are found to be mediating their toxicity is by generating an overwhelming amount of ROS, resulting in toxicity at target locations (Hwang et al., 2021; Khachatryan et al., 2011). An overwhelming surge of ROS generation in the target cells subsequently triggers a severe inflammatory cellular reaction, leading to further ROS generation. The coal dust has also been reported to have a ROS generation tendency at the target cells, which mediates their toxicity (Batool et al., 2020; Vallyathan et al., 1998; Zazouli et al., 2021). Usually, the pyrite (FeS_2) content of the coal dust is attributed to its ROS potential (Cohn et al., 2006; Zazouli et al., 2021). Some other studies do not agree that the pyrite content of coal dust is the reason for the ROS potential of coal dust (Zosky et al., 2021). Another mechanism attributed to the ROS generation by inhaled coal dust is through surface redox reactions catalyzed by metal ions, such as Cr, Co, Cd, Mn, Al, As, Pb, Cu, Zn, Sb etc., present in the coal dust (Zazouli et al., 2021). Molecular modeling of lignite coal shows that the molecular fragments are bounded to each other with the help of metal cations (Narayani and Zingaro Ralph, 1984). Notably, the clay mineral surfaces enriched with transition metal ions (such as Fe(III), Cu(II), Ni(II), Co(II), and Zn(II)) are found to be playing a positive role in the formation and fate of PAH-induced EPFR intermediates under environmentally relevant conditions (Jia et al., 2018). It will be an interesting task and a subject of future studies to understand the role of these metal ions and other minerals in the molecular structure of coal dust in affecting the EPFRs characteristics of coal dust.

The molecular structure of coal is strongly aromatic (Davidson, 1982). Most of the molecular structure of coal is carbon in different forms and representations (Mathews and Chaffee, 2012). This is why coal mainly has carbon-centered free radicals (although surrounded by heteroatoms). Given that the molecular structure of coal mainly comprises a number of aromatic systems, substituted by aliphatic groupings serving mainly as a linkage between the ordered regions (Given, 1959). Moreover, its aromaticity increases steadily with vitrinite reflectance and rank (Gorbaty et al., 1982). The higher conjugation and resonance effects in the aromatic structure of coal seem to be playing a major role in the stabilization of free radicals in coal dust. It can be seen in the present work that the lignite coal (low rank and less reflectance) has low free radical counts (Figs. 4, 7, 8, 10). This matches the fact that the lignite has a less aromatic structure and hence will have less concentration of stable free radicals. A special class of aromatic compounds termed polycyclic aromatic hydrocarbons (PAHs) is also found in coal dust, which is toxic and could convert to EPFRs under certain conditions (Achten and Hofmann, 2009; Sartorelli et al., 2001; Xu et al., 2022). Whereas the molecular structure of bituminous coal contains a much higher content of

aromatic, hydroaromatic and less heteroaromatic structures when compared to lignite coal. Because of increased conjugation and resonance, the stable free radical concentration of the bituminous coal dust is higher.

Apart from metal ions and pyrite, EPFRs present in the coal dust could be another major contributor to the ROS generation potential of coal dust. Exposure of BEAS-2B cells to combustion-generated particle systems containing EPFRs significantly increased (ROS) generation and decreased cellular antioxidants resulting in cell death (Balakrishna et al., 2009). Lavrent et al. observed that many hydroxyl radicals formed per EPFR (Khachatryan et al., 2011). They also observed a monotonic increase of the DMPO–OH spin adduct concentration with incubation time, suggesting a catalytic cycle of ROS formation. Another study found that surface-bound, rather than free, hydroxyl radicals were generated by a surface-catalyzed-redox cycle involving both the EPFRs and Cu(II)O (Khachatryan and Dellinger, 2011). Another study suggested that the EPFRs in $PM_{2.5}$ can generate significant levels of •OH without adding H_2O_2 (Gehling et al., 2014). Additionally, higher particle concentrations produced more hydroxyl radicals. Combustion-based EPFRs were found in $PM_{2.5}$ collected from Asian sandstorms, which were positively correlated with the oxidation potential of the host particulates (Chen et al., 2018).

Interestingly several of these and other works on analyzing the EPFRs in air pollution and combustion-based particulates studies have reported types of EPFRs similar to what was found in the present study. Fig. 11 compares the characteristics of EPFRs found in the coal dust in the present study with other similar studies (also check Table S9).

It was found in the present study that the EPFRs in the coal dust particles have a *g*-value in the range of 2.0029 to 2.0037. These *g*-values are attributed to organic free radicals (oxygenated carbon centered). Xu et al. reviewed 23 studies dealing with EPFRs in $PM_{2.5}$ and found that 16 out of these studies reported an average *g*-value between 2.003 and 2.004, mostly attributed to semiquinone radicals (Xu et al., 2019). Overall, they reported an averaged *g*-value of 1.9979–2.0091 for all 23 investigations analyzing types of EPFRs in $PM_{2.5}$. We clearly identified that the *g*-values of the coal dust found in the present study lie in the range mentioned in the $PM_{2.5}$. The highest spin count of 264 μmol/g was reported for $PM_{1.0}$ in Beijing, one order higher than what was observed for bituminous coal dust in the present study. The average concentration of EPFRs was around 2 μmol/g, slightly less than the EPFR concentration of lignite coal dust and one order less than the bituminous coal dust used in the present study (see Table S4). Chen et al. reported the source of EPFRs in atmospheric particulate matter (PM) of different particle sizes (<10 μm) in Linfen, a typical coal-burning city in China (Chen et al., 2020). They found that although the average *g*-values for EPFRs differ for large and small particles and depend on the season (summer or winter), they range between 2.0030 and 2.0037, which is similar to the observation in the present study. The EPFR concentration reported in their study ranges between 5.313×10^{-5} and 6×10^{-4} μmol/m^3. The *g*-values and the spin counts of EPFRs found in the present study are especially similar EPFRs formed through the combustion of organic materials such as wood, biochar, urban street dust, woodsmoke, wheat straw etc. (Dugas et al., 2016). Note that most of the ultrafine particles (similar to the nano-size coal dust used in the present study) released into the environment are generated in the combustion processes or result from secondary reactions involving combustion by-products (Lord et al., 2011). Filippi et al. identified EPFRs in indoor particulate matter, dust and on surfaces having g-values all ranging between 2.002 and 2.004, which is often associated with combustion processes (Filippi et al., 2022). Wildfire charcoals (Sigmund et al., 2021) and biochars-based EPFRs were also found to have similar characteristics to EPFRs in the present study (Odinga et al., 2020). EPFRs found in haze-associated atmospheres are also reported to have a g-value of 2.003–2.004 (indicating the existence of a mixture of oxygen-centered and carbon-centered semiquinone radicals or carbon-centered radicals with an adjacent oxygen atom), which is similar to the EPFRs found in the coal dust in the present study (Yang et al., 2017). The spin count reported in this study is in the range of 50.8–1034.36 μmol/g, which is several orders of magnitude higher than the spin counts of EPFRs observed in the present study. Air-Borne Soot Particles Generated by Burning Wood or Low-Maturity Coals also release EPFRs with g-values around 2.0033 (Jia et al., 2020). The same study evaluated the contribution of EPFRs in soot samples to the overall cytotoxicity by determining the cell viability in the presence or absence of a free radical scavenger (*N*-acetyl-L-cysteine, NAC). The results showed that the EPFRs (a similar type of EPFR found in the present study) contributed to the partial cytotoxicity of the soot particles (Jia et al., 2020). A key point to note is that the concentration of EPFRs in wood-burning (<0.166 μmol/g) and coal-burning soot (<0.174 μmol/g) was less compared to the present study. A higher concentration could have been more toxic, as demonstrated by Gehling et al. (Gehling et al., 2014). Kevin et al. generated EPFR of 1, 2 dichlorobenzenes formed by thermal reaction at 230 °C (DCB230) with silica particles (~200 nm dia.) containing 3 % CuO, which mimic those formed during combustion of chlorinated hydrocarbons and chlorine-containing fuels to understand the chemistry and biological actions of EPFRs (Lord et al., 2011). They

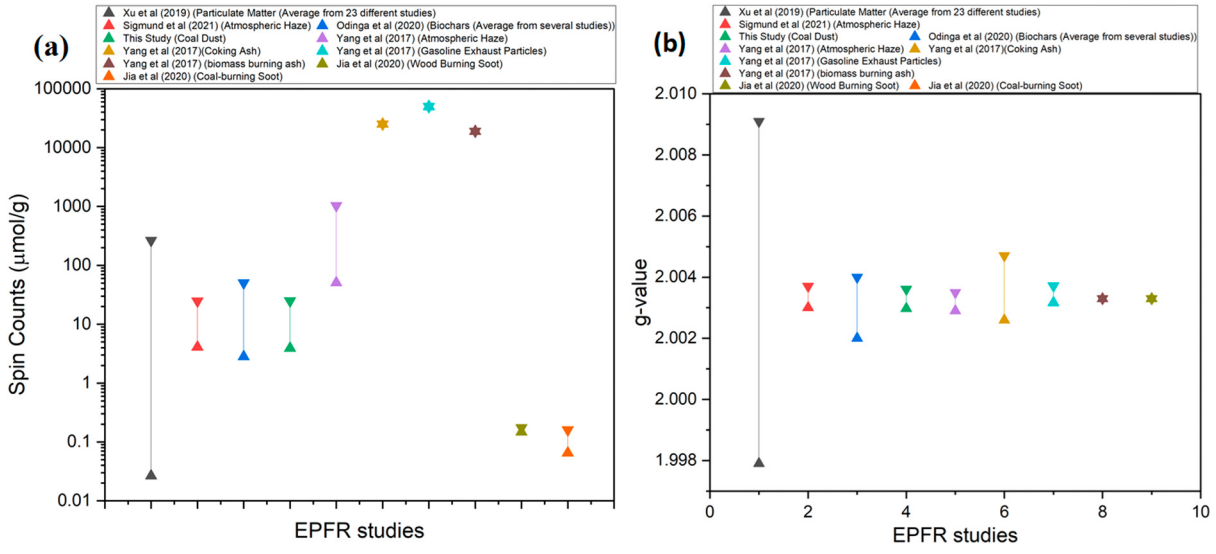

Fig. 11. (a) Comparison of EPFR spin counts from recent studies; (b) comparison of EPFR g-values from recent studies. It can be observed that the characteristics of CCEPFRs identified in the present study are similar to other studies.

observed that the instillation of EPFRs containing ultrafine DCB230 produces pulmonary and cardiac inflammation, decreases basal cardiac function in vivo and induces the expression of proinflammatory genes in the heart. This means that the EPFRs may affect cardiac function in healthy individuals and pose a special risk to individuals with ischemic heart disease. Ashlyn et al. exposed C57BL/6 male mice to DCB230 containing EPFRs for either 4 h or 4 h/day for 10 days and assessed their lung and vascular function (Harmon et al., 2021). They observed that the inhalation of EPFR-containing particulates led to decreased vascular responsiveness associated with an altered pulmonary function in the mice. Using engineered ultrafine DCB230 (which is a representative of combustion-generated particulate matter) containing EPFRs, Paul et al. showed their potential to substantially influence pulmonary development through induction of epithelial-to-mesenchymal transition (EMT), which may be important in determining the predisposition to asthma (Thevenot et al., 2013). Fahmy et al. engineered 2.5 μm surrogate EPFR-particle systems representative of combustion-generated EPFRs. In vitro, they found that EPFRs caused greater oxidative stress and reductions in cell viability as compared to control particles containing the organic precursor and no EPFRs (Fahmy et al., 2010). Neonatal exposure to EPFR-containing PM resulted in pulmonary oxidative stress, which further resulted in increased T_{regs} (regulatory T-cells) in the lungs and subsequent suppression of adaptive immune response to influenza (Lee et al., 2014). Particulate matter containing EPFRs is found to be related to adverse infant respiratory health effects (Saravia et al., 2013).

From the above discussion, EPFRs present in coal dust identified by this study are similar in characteristics to the EPFRs, which are found in combustion-generated particulates, $PM_{2.5}$, indoor dust, wildfires, biochar, haze etc. Furthermore, as described above, several studies demonstrated the health hazard potential of EPFRs found in combustion-generated particulates, which are almost identical to those found in respirable coal dust described in the present study. Another important point that needs to be discussed here is the reach and deposition of coal dust particles in the respiratory tract of humans. The human respiratory system is a long and complex track that undergoes several changes during each breathing cycle. The flow and deposition of coal dust particles depend upon several factors, such as particle size (Ou et al., 2020), hygroscopicity (R et al., 2014; Varghese and Gangamma, 2009), mixing state (Ching and Kajino, 2018) etc. Intuitively, smaller particles can penetrate deeper into the respiratory tract and reach the deepest lung region. Besides the discussed importance of size and material, nanoparticle biokinetics is also affected by other particle characteristics, such as the surface charge (zeta potential) and surface structures (Geiser and Kreyling, 2010). Correspondingly, depending upon the reach of the respirable coal dust, the EPFRs attached to them will impact the different regions of the respiratory system. It should be noted that the coal dust particles used in the present study are mainly of the order of a few 100 nm. EPFRs on particles of a similar size used in the present study, i.e., $EPFR_{0.2}$ (EPFRs on particulates <0.2 μm in size), were found to penetrate much deeper into alveoli altering the antioxidant capabilities (Thevenot et al., 2013). Whereas comparatively larger $EPFR_{2.5}$ (EPFRs on particulates <2.5 μm in size) generated H_2O_2 in the lungs of exposed neonatal animals. A study dealing with the size-resolved exposure risk of EPFRs in atmospheric aerosols found that the concentration of EPFRs on fine particles (<2.1 μm) is larger than on large particles (>2.1 μm) in summer and vice-versa in winter (Chen et al., 2020). They also mentioned that the upper respiratory tract is the area with the highest EPFR exposure. The risk of exposure is equivalent to that of 8 cigarettes per person per day for the trachea and alveoli exposed to EPFRs (Chen et al., 2020). Hygroscopicity or wettability of the coal dust could impact its size, as discussed in several ways (Asgharian, 2010; Davies et al., 2021; R et al., 2014). It is well known that the relative humidity inside the respiratory tract is dynamic and changes in every cycle depending on age, the activity of the individual and outside humidity (Bugarski and Gautam, 2001; Löndahl et al., 2010; Ohsaki et al., 2019; Youn et al., 2016). Moreover, the wettability of coal dust is directly proportional to its particle size (Wang et al., 2019) and inversely proportional to its carbon content (Xu et al., 2017). This suggests that the nano-size bituminous coal dust (which has larger carbon content, see Tables S2, S3 and Fig. S1) will be more hydrophobic in nature when compared to lignite coal dust. They will not easily increase in size because of less moisture adsorption on them. Due to less adsorption, their specific gravity will not change much. Hence, they will not easily agglomerate or get deposited unless they reach the deep, constrained region of the respiratory system. Because of this, EPFRs-packed bituminous coal dust will penetrate deeper regions of the human respiratory system. And we observed that the bituminous coal has a much higher concentration of EPFRs. Combining low wettability and higher EPFRs concentration in the higher rank coal might be the reason that higher-rank coal (with higher carbon content) is often found to be more correlated with their CWP potential (Attfield and Seixas, 1995; "Current intelligence bulletin 64: coal mine dust exposures and associated health outcomes - a review of information published since 1995.," 2020).

These studies discussed above to provide evidence that the nano-sized coal dust particles could carry EPFRs deeper into the respiratory system of humans and might be a contributing reason for CWP among coal miners. Also, it can be hypothesized that the nano-size bituminous coal dust could be more hazardous than the lignite as they have an order of magnitude higher EPFR concentration than lignite coal dust (Table S4). In a different study, coal mine dust was also found to generate hydroxyl radicals which are related to CWP (Dalal et al., 1995). The same study mentioned that the concentrations of surface iron in coal mine dust might be involved in generating increased levels of •OH radicals. As discussed earlier, the EPFRs in the coal dust could play a major role in mediating the generation of •OH radicals.

5. Summary and conclusions

In this study, we analyzed the EPFR characteristics of coal dust using EPR techniques and how the type and nature of coal influence these characteristics. We also discussed the possible ways these EPFRs in the coal dust could modulate the toxicity of coal dust in light of analogous studies conducted recently using particulates that had similar EPFR characteristics to that of coal dust in the present study. The key points can be summarized below:

- Coal dust contains free radicals in extremely large quantities, which could remain stable for several years and hence should be called as EPFRs.
- EPFRs in coal dust are mainly oxygenated carbon-centered in the bituminous coal dust, whereas a mixture of oxygenated or oxygen and carbon-centered in lignite coal dust. EPFR g-value decreases with the increasing carbon content of the coal.
- The EPFRs quantity (spin counts) increases with the carbon content and reflectance, suggesting that EPFR quantity is proportional to the degree of coalification the coal has undergone and that the coal dust from more mature coal has more EPFRs.
- Most of the particulate-based EPFRs discussed in the recent studies, whether the EPFRs are on organic compounds, haze, combustion-generated particulates, or wildfire-released particulates, are almost identical in characteristics to those of EPFRs analyzed in the coal dust in the present study.
- Considering the toxicity analysis of particulates containing EPFRs similar to those identified in the present study, it can be confidently hypothesized that the EPFRs in the coal dust might play a major role in modulating the coal dust toxicity.

In conclusion, we recommend future work should be conducted using in-vitro and in-vivo biological tests with coal dust particles studying EPFR characteristics as the indicator to firmly assess the role played by EPFRs in impacting coal dust toxicity. The most important aspect is to analyze the role of EPFR-loaded coal dust in mediating the inhalation toxicity of coal dust.

Glossary

CMDLD	Coal mine dust lung disease
CWP	Coal workers pneumoconiosis
EPFRs	Environmentally persistent free radicals
EPR	Electron paramagnetic resonance
PMF	Progressive massive fibrosis
ROS	Reactive oxygen species

CRediT authorship contribution statement

SL, JG and SA designed the research; SA and VK performed the experiments; SA analyzed and interpreted the data; SA drafted the manuscript. SL, VK, JB, SZ and SB gave feedback and contributed to the writing of the manuscript. All authors read and approved the final manuscript.

Data availability

Data will be made available on request.

Declaration of competing interest

The authors declare that they have no known competing financial interests or personal relationships that could have appeared to influence the work reported in this paper.

Acknowledgments

This work was financially supported by The National Institute of Occupational Safety and Health (NIOSH) under contract No. 75D30119C05128.

Appendix A. Supplementary data

Supplementary data to this article can be found online at https://doi.org/10.1016/j.scitotenv.2023.163163.

References

Achten, C., Hofmann, T., 2009. Native polycyclic aromatic hydrocarbons (PAH) in coals – a hardly recognized source of environmental contamination. Sci. Total Environ. 407, 2461–2473. https://doi.org/10.1016/J.SCITOTENV.2008.12.008.

Arangio, A.M., Tong, H., Socorro, J., Pöschl, U., Shiraiwa, M., 2016. Quantification of environmentally persistent free radicals and reactive oxygen species in atmospheric aerosol particles. Atmos. Chem. Phys. 16, 13105–13119. https://doi.org/10.5194/ACP-16-13105-2016.

Asgharian, B., 2010. A Model of Deposition of Hygroscopic Particles in the Human Lung. 38, pp. 938–947. https://doi.org/10.1080/027868290511236.

Attfield, M., Castranova, V., Hale, J.M., Suarthana, E., Thomas, K.C., Wang, M.L., 2011. Coal Mine Dust Exposures and Associated Health Outcomes; A Review of Information Published Since 1995.

Attfield, M.D., Seixas, N.S., 1995. Prevalence of pneumoconiosis and its relationship to dust exposure in a cohort of U.S. bituminous coal miners and ex-miners. Am. J. Ind. Med. 27, 137–151. https://doi.org/10.1002/AJIM.4700270113.

Balakrishna, S., Lomnicki, S., McAvey, K.M., Cole, R.B., Dellinger, B., Cormier, S.A., 2009. Environmentally persistent free radicals amplify ultrafine particle mediated cellular oxidative stress and cytotoxicity. Part Fibre Toxicol. 6, 1–14. https://doi.org/10.1186/1743-8977-6-11/FIGURES/9.

Batool, A.I., Naveed, N.H., Aslam, M., da Silva, J., Ur Rehman, M.F., 2020. Coal dust-induced systematic hypoxia and redox imbalance among coal mine workers. ACS Omega 5, 28204–28211. https://doi.org/10.1021/ACSOMEGA.0C03977.

Bugarski, A., Gautam, M., 2001. Size distribution and deposition in human respiratory tract_ particle mass and number. 4th International ETH-Conference on Nanoparticle Measurement, pp. 1–12.

Chen, Q., Sun, H., Song, W., Cao, F., Tian, C., Zhang, Y.L., 2020. Size-resolved exposure risk of persistent free radicals (PFRs) in atmospheric aerosols and their potential sources. Atmos. Chem. Phys. 20, 14407–14417. https://doi.org/10.5194/ACP-20-14407-2020.

Chen, Q., Wang, M., Sun, H., Wang, X., Wang, Y., Li, Y., Zhang, L., Mu, Z., 2018. Enhanced health risks from exposure to environmentally persistent free radicals and the oxidative stress of PM2.5 from Asian dust storms in Erenhot, Zhangbei and Jinan,China. Environ. Int. 121, 260–268. https://doi.org/10.1016/J.ENVINT.2018.09.012.

Ching, J., Kajino, M., 2018. Aerosol mixing state matters for particles deposition in human respiratory system. Sci. Rep. 8, 1–11. https://doi.org/10.1038/s41598-018-27156-z 2018 8:1.

Cohn, C.A., Laffers, R., Simon, S.R., O'Riordan, T., Schoonen, M.A.A., 2006. Role of pyrite in formation of hydroxyl radicals in coal: possible implications for human health. Part Fibre Toxicol. 3, 1–10. https://doi.org/10.1186/1743-8977-3-16/FIGURES/7.

Current intelligence bulletin 64: coal mine dust exposures and associated health outcomes - a review of information published since 1995. https://doi.org/10.26616/NIOSHPUB2011172.

Dalal, N.S., Jafari, B., Vallyathan, V., Petersen, M., Green, F.H.Y., 1991. Presence of stable coal radicals in autopsied coal miners'lungs and its possible correlation to coal workers'pneumoconiosis. Arch. Environ. Health 46, 366–372. https://doi.org/10.1080/00039896.1991.9934404.

Dalal, N.S., Newman, J., Pack, D., Leonard, S., Vallyathan, V., 1995. Hydroxyl radical generation by coal mine dust: possible implication to coal workers'pneumoconiosis (CWP). Free Radic. Biol. Med. 18, 11–20. https://doi.org/10.1016/0891-5849(94)E0094-Y.

Dalal, N.S., Suryan, M.M., Vallyathan, V., Green, F.H.Y., Jafari, B., Wheeler, R., 1989. Detection of reactive free radicals in fresh coal mine dust and their implication for pulmonary injury. Ann. Occup. Hyg. 33, 79–84. https://doi.org/10.1093/annhyg/33.1.79.

Davidson, R.M., 1982. Molecular structure of coal. Coal Sci., 83–160 https://doi.org/10.1016/B978-0-12-150701-5.50009-7.

Davies, J.F., Price, C.L., Choczynski, J., Kohli, R.K., 2021. Hygroscopic growth of simulated lung fluid aerosol particles under ambient environmental conditions. Chem. Commun. 57, 3243–3246. https://doi.org/10.1039/D1CC00066G.

Dellinger, B., Pryor, W.A., Cueto, R., Squadrito, G.L., Hegde, V., Deutsch, W.A., 2001. Role of free radicals in the toxicity of airborne fine particulate matter. Chem. Res. Toxicol. 14, 1371–1377. https://doi.org/10.1021/TX010050X/ASSET/IMAGES/LARGE/TX010050XF00005.JPEG.

Doney, B.C., Blackley, D., Hale, J.M., Halldin, C., Kurth, L., Syamlal, G., Laney, A.S., 2019. Respirable coal mine dust in underground mines, United States, 1982–2017. Am. J. Ind. Med. 62, 478–485. https://doi.org/10.1002/ajim.22974.

Dugas, T.R., Lomnicki, S., Cormier, S.A., Dellinger, B., Reams, M., 2016. Addressing emerging risks: scientific and regulatory challenges associated with environmentally persistent free radicals. Int. J. Environ. Res. Public Health 13. https://doi.org/10.3390/IJERPH13060573.

Fahmy, B., Ding, L., You, D., Lomnicki, S., Dellinger, B., Cormier, S.A., 2010. In vitro and in vivo assessment of pulmonary risk associated with exposure to combustion generated fine particles. Environ. Toxicol. Pharmacol. 29, 173. https://doi.org/10.1016/J.ETAP.2009.12.007.

Fan, L., Liu, S., 2021. Respirable nano-particulate generations and their pathogenesis in mining workplaces: a review. Int. J. Coal Sci. Technol., 1–20 https://doi.org/10.1007/s40789-021-00412-w.

Filippi, A., Sheu, R., Berkemeier, T., Pöschl, U., Tong, H., Gentner, D.R., 2022. Environmentally persistent free radicals in indoor particulate matter, dust, and on surfaces. Environ. Sci. Atmos. https://doi.org/10.1039/D1EA00075F.

Gehling, W., Khachatryan, L., Dellinger, B., 2014. Hydroxyl radical generation from environmentally persistent free radicals (EPFRs) in PM2.5. Environ. Sci. Technol. 48, 4266–4272. https://doi.org/10.1021/ES401770Y/SUPPL_FILE/ES401770Y_SI_001.PDF.

Geiser, M., Kreyling, W.G., 2010. Deposition and biokinetics of inhaled nanoparticles. Part Fibre Toxicol. https://doi.org/10.1186/1743-8977-7-2.

Given, P.H., 1959. Structure of bituminous coals: evidence from distribution of hydrogen. Nature 184, 980–981. https://doi.org/10.1038/184980a0 1959 184:4691.

Gorbaty, M.L., Larsen, J.W., Wender, Irving, Davidson, R.M., 1982. Coal Science. Academic Press.

Green, U., Aizenshtat, Z., Ruthstein, S., Cohen, H., 2012. Stable radicals formation in coals undergoing weathering: effect of coal rank. Phys. Chem. Chem. Phys. 14, 13046–13052.

Gurgueira, S.A., Lawrence, J., Coull, B., Krishna Murthy, G.G., González-Flecha, B., 2002. Rapid increases in the steady-state concentration of reactive oxygen species in the lungs and heart after particulate air pollution inhalation. Environ. Health Perspect. 110, 749–755. https://doi.org/10.1289/ehp.02110749.

Hall, N.B., Blackley, D.J., Halldin, C.N., Laney, A.S., 2019. Current review of pneumoconiosis among US coal miners. Curr. Environ. Health Rep. https://doi.org/10.1007/s40572-019-00237-5.

Harmon, A.C., Noël, A., Subramanian, B., Perveen, Z., Jennings, M.H., Chen, Y.F., Penn, A.L., Legendre, K., Paulsen, D.B., Varner, K.J., Dugas, T.R., 2021. Inhalation of particulate matter containing free radicals leads to decreased vascular responsiveness associated with an altered pulmonary function. Am. J. Physiol. Heart Circ. Physiol. 321, H667–H683. https://doi.org/10.1152/AJPHEART.00725.2020/ASSET/IMAGES/LARGE/AJPHEART.00725.2020_F009.JPEG.

Hwang, B., Fang, T., Pham, R., Wei, J., Gronstal, S., Lopez, B., Frederickson, C., Galeazzo, T., Wang, X., Jung, H., Shiraiwa, M., 2021. Environmentally persistent free radicals, reactive oxygen species generation, and oxidative potential of highway PM2.5. ACS Earth Space Chem. 5, 1865–1875. https://doi.org/10.1021/ACSEARTHSPACECHEM.1C00135/ASSET/IMAGES/LARGE/SP1C00135_0005.JPEG.

Jia, H., Li, Shuaishuai, Wu, L., Li, Shiqing, Sharma, V.K., Yan, B., 2020. Cytotoxic free radicals on air-borne soot particles generated by burning wood or low-maturity coals. Environ. Sci. Technol. 54, 5608–5618. https://doi.org/10.1021/ACS.EST.9B06395/ASSET/IMAGES/LARGE/ES9B06395_0002.JPEG.

Jia, H., Zhao, S., Shi, Y., Zhu, L., Wang, C., Sharma, V.K., 2018. Transformation of polycyclic aromatic hydrocarbons and formation of environmentally persistent free radicals on modified montmorillonite: the role of surface metal ions and polycyclic aromatic hydrocarbon molecular properties. Environ. Sci. Technol. 52, 5725–5733. https://doi.org/10.1021/ACS.EST.8B00425/ASSET/IMAGES/LARGE/ES-2018-00425M_0004.JPEG.

Khachatryan, L., Dellinger, B., 2011. Environmentally persistent free radicals (EPFRs)-2. Are free hydroxyl radicals generated in aqueous solutions? Environ. Sci. Technol. 45, 9232–9239. https://doi.org/10.1021/ES201702Q/SUPPL_FILE/ES201702Q_SI_001.PDF.

Khachatryan, L., Vejerano, E., Lomnicki, S., Dellinger, B., 2011. Environmentally persistent free radicals (EPFRs). 1. Generation of reactive oxygen species in aqueous solutions. Environ. Sci. Technol. 45, 8559–8566. https://doi.org/10.1021/ES201309C/ASSET/IMAGES/LARGE/ES-2011-01309C_0005.JPEG.

Laney, A.S., Weissman, D.N., 2014. Respiratory diseases caused by coal mine dust. Journal of Occupational and Environmental Medicine. Lippincott Williams and Wilkins, pp. S18–S22 https://doi.org/10.1097/JOM.0000000000000260.

Lee, G.I., Saravia, J., You, D., Shrestha, B., Jaligama, S., Hebert, V.Y., Dugas, T.R., Cormier, S.A., 2014. Exposure to combustion generated environmentally persistent free radicals enhances severity of influenza virus infection. Part Fibre Toxicol. 11, 1–10. https://doi.org/10.1186/S12989-014-0057-1/FIGURES/4.

Li, D., Liao, Y., 2018. Spatial characteristics of heavy metals in street dust of coal railway transportation hubs: a case study in Yuanping, China. Int. J. Environ. Res. Public Health 15. https://doi.org/10.3390/IJERPH15122662.

Li, F., Li, X., Hou, L., Shao, A., 2018. Impact of the coal mining on the spatial distribution of potentially toxic metals in farmland tillage soil. Sci. Rep. 8, 1–10. https://doi.org/10.1038/s41598-018-33132-4 2018 8:1.

Liu, J., Jiang, X., Shen, J., Zhang, H., 2014. Chemical properties of superfine pulverized coal particles. Part 1. Electron paramagnetic resonance analysis of free radical characteristics. Adv. Powder Technol. 25, 916–925. https://doi.org/10.1016/J.APT.2014.01.021.

Liu, T., Liu, S., 2020. The impacts of coal dust on miners'health: a review. Environ. Res. https://doi.org/10.1016/j.envres.2020.109849.

Löndahl, J., Massling, A., Pagels, J., Swietlicki, E., Vaclavik, E., Loft, S., 2010. Size-resolved Respiratory-tract Deposition of Fine and Ultrafine Hydrophobic and Hygroscopic Aerosol Particles During Rest and Exercise. 19, pp. 109–116. https://doi.org/10.1080/08958370601051677.

Lord, K., Moll, D., Lindsey, J.K., Mahne, S., Raman, G., Dugas, T., Cormier, S., Troxlair, D., Lomnicki, S., Dellinger, B., Varner, K., 2011. Environmentally persistent free radicals decrease cardiac function before and after ischemia/reperfusion injury in vivo. J. Recept. Signal Transduct. Res. 31, 157. https://doi.org/10.3109/10799893.2011.555767.

Mathews, J.P., Chaffee, A.L., 2012. The molecular representations of coal – a review. Fuel 96, 1–14. https://doi.org/10.1016/J.FUEL.2011.11.025.

Narayani, M., Zingaro Ralph, A., 1984. Some structural features of a Wilcox lignite. ACS Symp. Ser. 264, 133–144.

Odinga, E.S., Waigi, M.G., Gudda, F.O., Wang, J., Yang, B., Hu, X., Li, S., Gao, Y., 2020. Occurrence, formation, environmental fate and risks of environmentally persistent free radicals in biochars. Environ. Int. 134, 105172. https://doi.org/10.1016/J.ENVINT.2019.105172.

Ohsaki, S., Mitani, R., Fujiwara, S., Nakamura, H., Watano, S., 2019. Effect of particle-wall interaction and particle shape on particle deposition behavior in human respiratory system. Chem. Pharm. Bull. (Tokyo) 67, 1328–1336. https://doi.org/10.1248/CPB.C19-00693.

Okayama, Y., Kuwahara, M., Suzuki, A.K., Tsubone, H., 2006. Role of reactive oxygen species on diesel exhaust particle-induced cytotoxicity in rat cardiac myocytes. J. Toxicol. Environ. Health A 69, 1699–1710. https://doi.org/10.1080/15287390600631078.

Ou, C., Hang, J., Deng, Q., 2020. Particle deposition in human lung airways: effects of airflow, particle size, and mechanisms. Aerosol Air Qual. Res. 20, 2846–2858. https://doi.org/10.4209/AAQR.2020.02.0067.

Pavan, C., Santalucia, R., Leinardi, R., Fabbiani, M., Yakoub, Y., Uwambayinema, F., Ugliengo, P., Tomatis, M., Martra, G., Turci, F., Lison, D., Fubini, B., 2020. Nearly free surface silanols are the critical molecular moieties that initiate the toxicity of silica particles. Proc. Natl. Acad. Sci. U. S. A. 117, 27836–27846. https://doi.org/10.1073/PNAS.2008006117/-/DCSUPPLEMENTAL.

Pavlovic, J., Hopke, P.K., 2010. Detection of radical species formed by the ozonolysis of α-pinene. J. Atmos. Chem. 66, 137–155. https://doi.org/10.1007/S10874-011-9197-Y/FIGURES/6.

Petrakis, Leon, Grandy, D.W., 1978. Electron spin resonance spectrometric study of free radicals in coals. Anal. Chem. 50, 303–308. https://doi.org/10.1021/AC50024A034.

Petsonk, E.L., Rose, C., Cohen, R., 2013. Coal mine dust lung disease: new lessons from an old exposure. Am. J. Respir. Crit. Care Med. 187, 1178–1185. https://doi.org/10.1164/RCCM.201301-0042CI/SUPPL_FILE/DISCLOSURES.PDF.

Pilawa, B., Więckowski, A.B., 2007. Groups of paramagnetic centres in coal samples with different carbon contents. Res. Chem. Intermed. 33, 825–839. https://doi.org/10.1163/156856707782169336 2007 33:8.

Pilawa, B., Więckowski, A.B., Wachowska, H., Kozłowski, M., 1998. E.p.r. searches of correlations between paramagnetic centre behaviour and chemical structure of reductively alkylated flame coal. Fuel 77, 1561–1567. https://doi.org/10.1016/S0016-2361(98)00099-4.

Proximate Analysis, 2015. Handbook of Coal Analysis, pp. 116–143 https://doi.org/10.1002/9781119037699.CH5.

R, W.-H., G, F., W, H., 2014. Calculation of hygroscopic particle deposition in the human lung. Inhal. Toxicol. 26, 193–206. https://doi.org/10.3109/08958378.2013.876468.

Saravia, J., Lee, G.I., Lomnicki, S., Dellinger, B., Cormier, S.A., 2013. Particulate matter containing environmentally persistent free radicals and adverse infant respiratory health effects: a review. J. Biochem. Mol. Toxicol. 27, 56–68. https://doi.org/10.1002/JBT.21465.

Sartorelli, P., Montomoli, L., Sisinni, A.G., Bussani, R., Cavallo, D., Foá, V., 2001. Dermal exposure assessment of polycyclic aromatic hydrocarbons: in vitro percutaneous penetration from coal dust. Toxicol. Ind. Health 17, 17–21. https://doi.org/10.1191/0748233701th092oa.

Sigmund, G., Santín, C., Pignitter, M., Tepe, N., Doerr, S.H., Hofmann, T., 2021. Environmentally persistent free radicals are ubiquitous in wildfire charcoals and remain stable for years. Commun. Earth Environ. 2, 1–6. https://doi.org/10.1038/s43247-021-00138-2 2021 2:1.

Speight, J.G., 2015. Handbook of Coal Analysis. https://doi.org/10.1002/9781119037699.

Squadrito, G.L., Cueto, R., Dellinger, B., Pryor, W.A., 2001. Quinoid redox cycling as a mechanism for sustained free radical generation by inhaled airborne particulate matter. Free Radic. Biol. Med. 31, 1132–1138. https://doi.org/10.1016/S0891-5849(01)00703-1.

Thevenot, P.T., Saravia, J., Jin, N., Giaimo, J.D., Chustz, R.E., Mahne, S., Kelley, M.A., Hebert, V.Y., Dellinger, B., Dugas, T.R., DeMayo, F.J., Cormier, S.A., 2013. Radical-containing ultrafine particulate matter initiates epithelial-to-mesenchymal transitions in airway epithelial cells. Am. J. Respir. Cell Mol. Biol. 48, 188–197. https://doi.org/10.1165/RCMB.2012-0052OC.

Vallyathan, V., Shi, X., Castranova, V., 1998. Reactive oxygen species: their relation to pneumoconiosis and carcinogenesis. Environ. Health Perspect. 106, 1151. https://doi.org/10.2307/3433978.

Varghese, S.K., Gangamma, S., 2009. Particle deposition in human respiratory system: deposition of concentrated hygroscopic aerosols. Inhal. Toxicol. 21, 619–630. https://doi.org/10.1080/08958370802380792.

Wang, P., Tan, X., Zhang, L., Li, Y., Liu, R., 2019. Influence of particle diameter on the wettability of coal dust and the dust suppression efficiency via spraying. Process Saf. Environ. Prot. 132, 189–199. https://doi.org/10.1016/J.PSEP.2019.09.031.

Wang, P., Thevenot, P., Saravia, J., Ahlert, T., Cormier, S.A., 2011. Radical-containing particles activate dendritic cells and enhance Th17 inflammation in a mouse model of asthma. Am. J. Respir. Cell Mol. Biol. 45, 977–983. https://doi.org/10.1165/RCMB.2011-0001OC.

Xu, B., Liu, F., Alfaro, D., Jin, Z., Liu, Yingying, Liu, Yuan, Zhou, Z., Zhang, J., 2022. Polycyclic aromatic hydrocarbons in fine road dust from a coal-utilization city: spatial distribution, source diagnosis and risk assessment. Chemosphere 286, 131555. https://doi.org/10.1016/J.CHEMOSPHERE.2021.131555.

Xu, C., Wang, D., Wang, H., Xin, H., Ma, L., Zhu, X., Zhang, Y., Wang, Q., 2017. Effects of chemical properties of coal dust on its wettability. Powder Technol. 318, 33–39. https://doi.org/10.1016/J.POWTEC.2017.05.028.

Xu, M., Wu, T., Tang, Y.T., Chen, T., Khachatryan, L., Iyer, P.R., Guo, D., Chen, A., Lyu, M., Li, J., Liu, J., Li, D., Zuo, Y., Zhang, S., Wang, Y., Meng, Y., Qi, F., 2019. Environmentally persistent free radicals in PM2.5: a review. Waste Dispos. Sustain. Energy 1, 177–197. https://doi.org/10.1007/S42768-019-00021-Z/FIGURES/7.

Yang, L., Liu, G., Zheng, M., Jin, R., Zhu, Q., Zhao, Y., Wu, X., Xu, Y., 2017. Highly elevated levels and particle-size distributions of environmentally persistent free radicals in haze-associated atmosphere. Environ. Sci. Technol. 51, 7936–7944. https://doi.org/10.1021/ACS.EST.7B01929/ASSET/IMAGES/LARGE/ES-2017-01929G_0005.JPEG.

Youn, J., Csavina, J., Rine, K.P., Shingler, T., Taylor, M.P., Sáez, A.E., Betterton, E.A., Sorooshian, A., 2016. Hygroscopic properties and respiratory system deposition behavior of particulate matter emitted by mining and smelting operations. Environ. Sci. Technol. 50, 11706. https://doi.org/10.1021/ACS.EST.6B03621.

Zazouli, M.A., Dehbandi, R., Mohammadyan, M., Aarabi, M., Dominguez, A.O., Kelly, F.J., Khodabakhshloo, N., Rahman, M.M., Naidu, R., 2021. Physico-chemical properties and reactive oxygen species generation by respirable coal dust: implication for human health risk assessment. J. Hazard. Mater. 405. https://doi.org/10.1016/J.JHAZMAT.2020.124185.

Zhang, R., Liu, S., Zheng, S., 2021. Characterization of nano-to-micron sized respirable coal dust: particle surface alteration and the health impact. J. Hazard. Mater. 413, 125447. https://doi.org/10.1016/j.jhazmat.2021.125447.

Zhang, Y., Zhang, J., Li, Y., Gao, S., Yang, C., Shi, X., 2021. Oxidation characteristics of functional groups in relation to coal spontaneous combustion. ACS Omega 6, 7669–7679. https://doi.org/10.1021/ACSOMEGA.0C06322.

Zhao, T., Yang, S., Hu, X., Song, W., Cai, J., Xu, Q., 2020. Restraining effect of nitrogen on coal oxidation in different stages: non-isothermal TG-DSC and EPR research. Int. J. Min. Sci. Technol. 30, 387–395. https://doi.org/10.1016/J.IJMST.2020.04.008.

Zhou, B., Liu, Q., Shi, L., Liu, Z., 2019. Electron spin resonance studies of coals and coal conversion processes: a review. Fuel Process. Technol. https://doi.org/10.1016/j.fuproc.2019.01.011.

Zosky, G.R., Bennett, E.J., Pavez, M., Beamish, B.B., 2021. No association between pyrite content and lung cell responses to coal particles. Sci. Rep. 11, 1–8. https://doi.org/10.1038/s41598-021-87517-z 2021 11:1.